ASD-TR-69-105

SENSITIVITY OF FATIGUE DAMAGE CALCULATIONS TO THE STRESS INCREMENT SIZE AND DIGITAL RESOLUTION OF LOAD FACTOR DATA

AD 864716

GEORGE J. ROTH

University of Dayton Research Institute

TECHNICAL REPORT ASD-TR-69-105

SEPTEMBER 1969

This document is subject to special export controls and each transmittal to foreign governments or foreign nationals may be made only with prior approval of the Deputy for Engineering, Aeronautical Systems Division, Wright-Patterson Air Force Base, Ohio 45433.

DEPUTY FOR ENGINEERING
AERONAUTICAL SYSTEMS DIVISION
AIR FORCE SYSTEMS COMMAND
WRIGHT-PATTERSON AIR FORCE BASE, OHIO 45433

NOTICE

100 - December 1969 - CO455 - 101-2213

ASD-TR-69-105

SENSITIVITY OF FATIGUE DAMAGE CALCULATIONS TO THE STRESS INCREMENT SIZE AND DIGITAL RESOLUTION OF LOAD FACTOR DATA

GEORGE J. ROTH

University of Dayton Research Institute

FOREWORD

This final report on the Sensitivity of Fatigue Damage Calculations to the Stress Increment Size and Digital Resolution of Load Factor Data was prepared by the Aerospace Mechanics Research Group of the University of Dayton Research Institute, Dayton, Ohio, under Air Force Contract F33657-67-C-0140-Amendment 003. This study was initiated and monitored by Mr. Gary Walker, ASNFS-20, Deputy for Engineering, Aeronautical Systems Division, Air Force Systems Command, Wright-Patterson Air Force Base, Ohio.

The work reported herein was accomplished during the period 1 February 1969 to 1 April 1969 by UDRI under the general supervision of Mr. Dale H. Whitford. This report was submitted by the author on July 25, 1969.

The author gratefully acknowledges the cooperation and assistance provided by Mr. Walker, the personnel of the ASD Computer Facilities, and associates at the University of Dayton who provided the computer programming.

This technical report has been reviewed and is approved.

Glenn Purkey

Glenn Purkey
Chief, Structures Division
Air Frames Subsystem Engineering

ABSTRACT

Fatigue damage calculations using Miner's cumulative damage rule were performed to determine the trade-off relationship between the number of mean and alternating stress intervals used to represent a load spectrum. Results indicate that if more than 5 mean stress intervals and more than 30 alternating stress intervals are used, the error in the calculations will be less than 2%.

Also presented are results showing the effect that the number of digital binary bits used to represent loads data has on the calculated fatigue damage. These results indicate that the minimum resolution for the ASIP recorder should be 8 digital bits.

TABLE OF CONTENTS

LIST OF ILLUSTRATIONS

LIST OF TABLES

SECTION I

INTRODUCTION

1. Historical Background

Because of the rapid technological advances that have been made in the aeronautical sciences since the first flight in 1903, it has often been technically possible to build an aircraft capable of flying in a new environment without having a complete understanding of the environment and its effects on an aircraft. Thus, since the earliest days of flying, aircraft have been plagued with structural failures because adequate design criteria were not available. The Air Force has recognized this inadequacy and for the last twenty years has been conducting studies of the atmosphere and the response of aircraft to atmospheric turbulence and pilot induced maneuvers. Most of these research efforts have involved the measurement of the gust and maneuver response of aircraft while flying normal operational missions.

In 1958, the B-47 fatigue failures emphasized that structural design criteria was still inadequate, and in June, approval was given by the Air Force to proceed with a major Aircraft Structural Integrity Program (ASIP). There have been a number of refinements of this program, and today the specific program objectives are:[1]

(1) To establish, evaluate, and substantiate structural integrity (airframe strength and service life) of aircraft systems.

(2) To continually reevaluate the structural integrity program by utilizing inputs from operational usage.

(3) To develop statistical techniques for the evaluation of operational usage and for logistic support (maintenance, inspection, supplies).

(4) To develop and incorporate improved structural criteria and methods of design, evaluation, and substantiation of aircraft systems.

Since the establishment of ASIP it has been a basic requirement to obtain flight loads data of various types from each operational fleet. Early plans suggested that the measurements of airspeed, altitude, and normal load factor data should be obtained from 20% of each fleet in the Air Force inventory for an extended period of time. It was recognized that the sheer magnitude of such a program would require the development of new systems for recording and automatically processing the data. In 1958 such a system was not available, and hence the obtaining of meaningful design criteria was limited to that which could be obtained by slow, relatively costly manual data processing methods.

It was recognized early that the magnetic tape recording technique would provide the data in a form that was capable of being processed automatically, but the specifications for size, weight, length of recording time, and accuracy were beyond the state of the art. Various hardware development programs were initiated in the 1960's, and the gap between the specifications and the state of the art closed.

In May 1965, the San Antonio Air Materiel Area initiated a B-58 Service Life Monitoring Program designed to monitor the fatigue damage accumulated by every B-58 aircraft at a number of fatigue critical points. A part of this program included the recording of eight measurements of stress and the measurement of airspeed, load factor, and altitude (VGH) from four aircraft flying operational missions. The stress data were subsequently converted to fatigue damage rates which were compared to those generated from the original aircraft design criteria. An FM tape recording system and automatic data processing system was developed.[2] This was the first use of such a system for a large scale ASIP effort, and the feasibility of accomplishing the ASIP objectives with an automated system was proved.

The impact of this evolution in recording and data processing in the short time from 1962 to 1965 is graphically portrayed by comparing the systems used for the B-52[3] and the B-58 Service Life Monitoring Programs.

Over a two year period, more than 10,000,000 data points were processed by manual and semi-automatic methods on the B-52 program, whereas on the B-58 program about 8,000,000 data points are processed automatically in less than 30 minutes in a much more complex form. This B-58 instrumentation and data processing system is still in use and is satisfying all ASIP requirements.

By 1968 a number of digital magnetic tape recorders which appeared to fulfill ASIP specifications were presented to the Air Force for evaluation. Before initiating a competitive procurement, the Air Force decided to evaluate one of the digital tape recorders by comparing it with the B-58 FM tape recorder. Thus, during May and June of 1968, the test digital recorder was installed next to the regular FM recorder in one B-58 aircraft, and these instruments were used to record simultaneously the data from the same set of strain gages and VGH transducers. These two sets of data were processed automatically to identical formats so that the performance of the two systems could be compared.

It was hoped that the digital recorder would provide acceptable results because of its simplicity and reliability of operation, compared to an FM system, and because its recorded tapes could be designed to be read directly by the computer. (The data from an FM tape must first be processed on the ground through a complex analog to digital conversion system before the data are capable of being read by a digital computer.)

As a result of the analog to digital conversion required by the FM-recorded data, there was a basic difference in the data resolution of the converted tape from the FM recorder and the tape obtained directly from the digital recorder being evaluated. Air Force specifications indicated that the resolution of the digital recorder should be such that the full scale of a given measurement would vary from zero to a number represented by six binary bits (i.e., the full scale range varied from 0 to 63 units). On the other hand, the analog to digital converter used to convert the FM tape to a computercompatible tape represented each digital measurement by an eleven-bit number, and the full scale range varied from 0 to 2047 units. This 11-bit digitization is a basic unalterable characteristic of the machine. The significance of this difference in resolution is shown in the following example. Assume the full scale range of a normal load factor measurement varies from 0 to 3 g. Then, 11-bit data would be resolved in increments of $3g/2047 = 0.00146$ g, whereas 6-bit data would be resolved in increments of $3g/63 = 0.0476$ g. For a measurement of 3 g, the resolution error in terms of percent of the measurement would be 0.048% for the 11-bit recorder and 1.58% for the 6-bit recorder. However, for a measurement of 0.5 g the resolution increment remains the same but the error in terms of percent of the measurement would be 0.29% for the 11-bit data and 9.5% for the 6-bit data. Figure 1 is a plot of the resolution error vs the magnitude of a measurement for 11, 10, 9, 8, 7, and 6-bit data.

The Air Force was particularly interested in the performance of the specific digital recorder which was used in the evaluation on the B-58 aircraft because that digital recorder was built in compliance with existing Air Force specifications. Thus, the B-58 test provided a means for evaluating the capability of the Air Force specification (MIL-R-38435) to provide a satisfactory system for measuring strain and load factor data that are used in cumulative fatigue damage computations.

The results of this recorder evaluation[4] were not encouraging, and in particular it appeared that 6-bit data specified for the ASIP recorder probably would not be adequate for fatigue computations for bomber and transport aircraft. For fighter or other high load factor type aircraft, the 6-bit resolution appeared to be adequate if not much computation is to be done with the data. Thus, it was recommended that a study be conducted prior to the initiation of recorder procurement action to determine the sensitivity of cumulative fatigue computations to the digital resolution of the data input to the computations. Recommendations also were made to study the effect of instrumentation drift on fatigue computations. This report contains the results of that study.

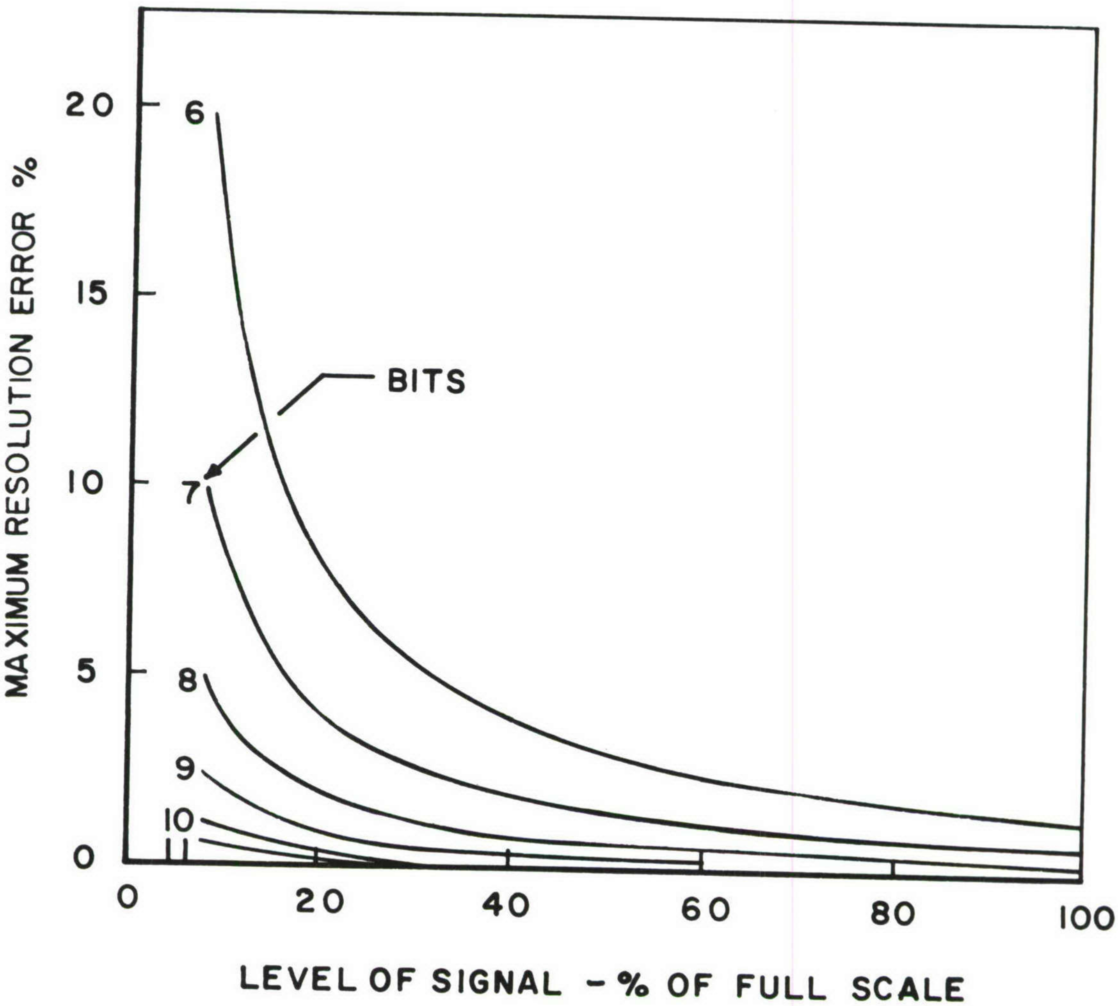

Figure 1. Maximum Resolution Error vs Signal Level for Various Digital Bits of Resolution

B. Objectives

The purpose of this program was to develop a basis for specifying the digital resolution and instrumentation drift characteristics required for the ASIP recorder. Specifically, the objectives were:

(1) to determine the error sensitivity of cumulative fatigue damage computations to the number of alternating stress and mean stress class intervals;

(2) to determine the adequate digital resolution of the recorded data for fatigue analysis computations if the instrumentation is not drifting;

(3) to determine the effect of instrumentation drift on required digital resolution.

SECTION II

CUMULATIVE DAMAGE SENSITIVITY STUDY

A. Miner's Cumulative Damage Theory

Miner's Cumulative Damage Theory[5] was used for this study because it is the most widely used fatigue analysis method by the aerospace industry. Miner's theory simply states that cumulative fatigue damage, the fraction of life used up by application of stress cycles of any amplitude, is just the ratio of the number of applied stress cycles to the number of stress cycles that would cause failure at a given amplitude. When different amplitude cycles are mixed together, failure occurs when the fractions of life expended at each amplitude add up to one[6]. Thus,

$$D = \sum_{i=1}^{k} \frac{n_i}{N_i} \tag{1}$$

where

- D is the fraction of life used up by the applied stress spectrum,
- n_i is the number of alternating stress cycles at stress amplitude i that are applied in a stress spectrum,
- N_i is the number of stress cycles required to cause failure at stress amplitude i, and
- k is the total number of stress amplitudes encompassing the applied stress spectrum.

The following derivation of Equation 1 by Kaechele[6] is presented to indicate the way in which the alternating stress interval size affects the accuracy of Equation 1. The applied stress spectrum is often specified in the form of a series of cumulative frequency curves representing the complete flight regume of an aircraft. A typical applied stress spectrum for one flight regime is shown in Figure 2. This graph is merely a plot of the cumulative

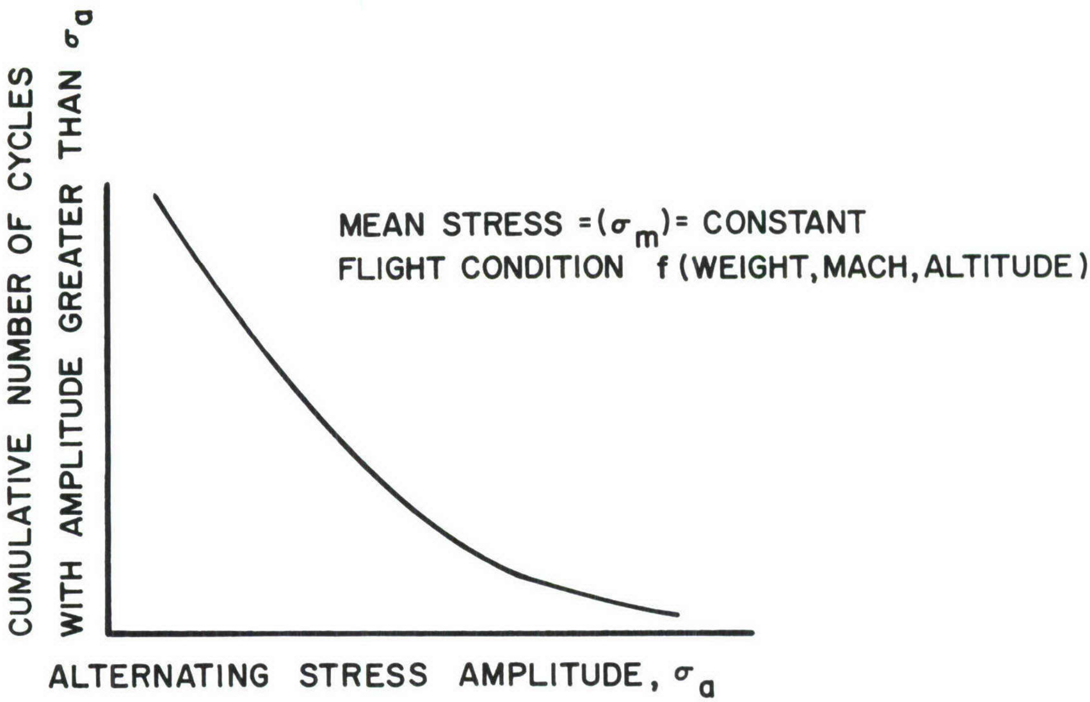

Figure 2. Typical Cumulative Stress Spectrum

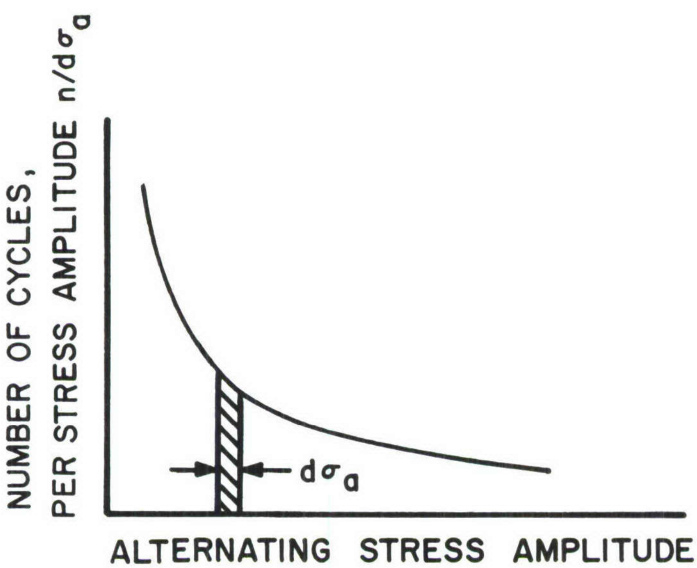

Figure 3. Number of Cycles Applied at Each Alternating Stress Level

number of stress cycles greater than the magnitude of alternating stress plotted on the abscissa. This curve represents the expected stress spectra for flight in a regime specified by a given combination of gross weight, Mach number, and altitude. Thus, the mean stress would be constant for the curve in Figure 2, and similar curves representing the entire range of mean stresses and flight regimes of the aircraft would also be required.

Since in using Miner's theory it is necessary to know the number of cycles of alternating stress (n_i) at each alternating stress level σ_{a_i}, the frequency distribution of the stress spectrum (Figure 3) is generated by plotting the absolute value of the slope of Figure 2 versus the alternating stress amplitude. Thus, the incremental area of Figure 3 represents the number of stress cycles having amplitudes in the interval between σ_a and $(\sigma_a + d\sigma_a)$.

The number of stress cycles required to fail a given material or structure as a function of stress level is determined empirically and is plotted in the form of an S-N curve such as the one shown in Figure 4. Note that this curve is highly non-linear. For convenience, the S-N curve is plotted here on linear axes with the axes reversed from the conventional form.

Figure 5 is a damage density plot which is derived by dividing pairs of ordinate values from Figures 3 and 4 which have the same value of alternating stress. This curve shows the amount of damage produced at the various levels of alternating stress. Then, the total damage for the complete stress spectrum of Figure 2 would be

$$D = \int \left(\frac{n/N}{d\sigma_a} \right) d\sigma_a \qquad (2)$$

which for a finite summation can be expressed in the familiar form of Equation 1.

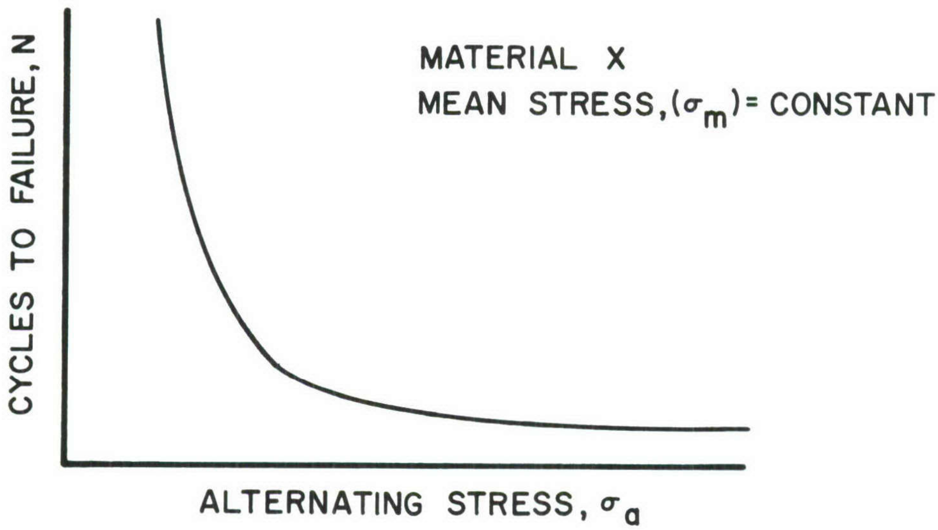

Figure 4. Typical S-N Curve for a Given Material and Mean Stress Level

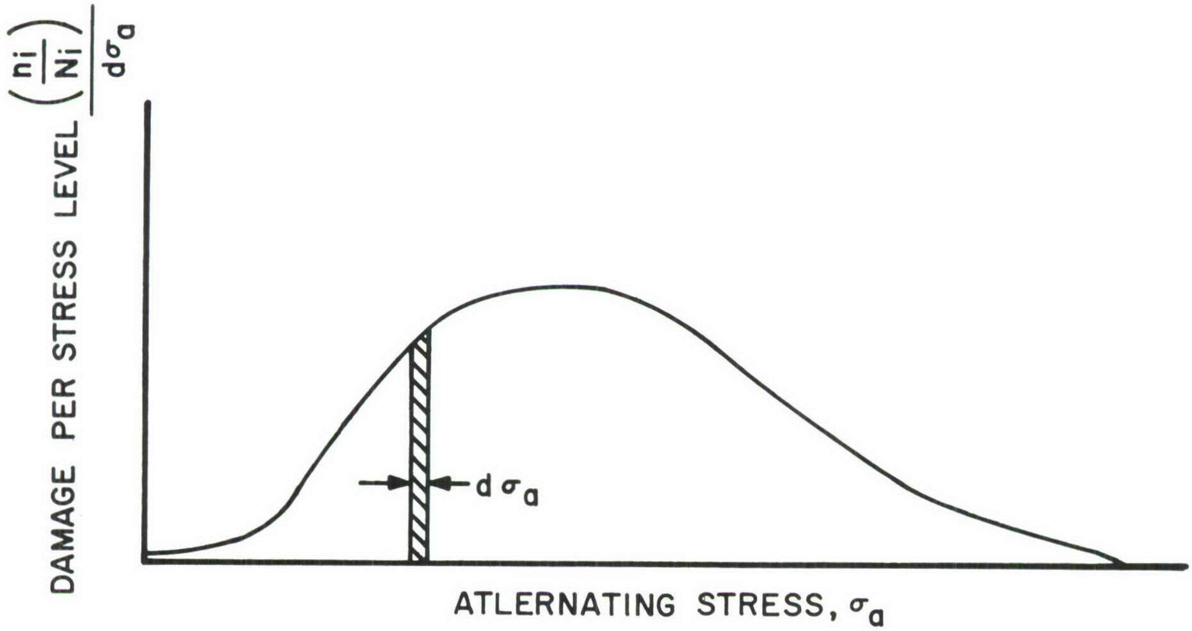

Figure 5. Damage Density Plot

Because of the empirical nature of the S-N curve (Figure 4), the damage integration is usually accomplished by use of numerical methods using Equation 1 rather than by use of Equation 2. Thus, one can readily see that care must be exercised to assure the proper selection of the size of the stress increment $\Delta\sigma_a$ in order to accomplish the integration of Equation 2 accurately.

In addition to the selection of the proper size of the alternating stress increment $\Delta\sigma_a$, one must also consider the size of the mean stress interval $\Delta\sigma_m$. The variation of the S-N curve with mean stress has marked effects on the damage caused by a given alternating stress spectrum. Thus, in this study the effect of the variation in mean stress and alternating stress interval size was examined in order to ascertain the combined effect of the incremental size of these parameters on the accuracy of a cumulative fatigue damage computation.

B. Analytical Procedures

The analytical procedure included the following steps: (1) selecting a stress spectrum that was representative of realistic aircraft stress experience at fatigue critical locations; (2) selecting S-N curves that were representative of those used for aircraft design and analysis; (3) computing fatigue damage for various combinations of $\Delta\sigma_a$ and $\Delta\sigma_m$ increment sizes; and (4) comparing the various damage computations to a standard which most nearly represented the exact integration of the damage equation.

1. Aircraft and Stress Spectra Selection

The B-58 and the F-105 aircraft were selected as examples for this study because information concerning the stress spectrum, operational regime, structural response, and fatigue characteristics was available. Primary emphasis was placed upon one of the low altitude gust spectra of the B-58 and on the maneuver spectrum of the F-105D.

Two critical fatigue points were selected for study on the B-58: the aft inboard wheel well corner on the lower wing surface (Control Point 1) and the intersection of the inboard pylon and the front wing spar (Control Point 10). A gust spectrum that was representative of aircraft flight at an altitude of 1000 ft and a Mach number of 0.91 also was selected.

The critical point for the F-105D was the top cover skin at Fuselage Station 509, and a measured maneuver spectrum representative of operation at 7000 ft and a Mach number of 0.92 was used.

2. S-N Curves

Since the shape of the S-N curve affects damage computation accuracy, a number of different stress spectra were selected so that different areas of the S-N curves would be investigated. Also, three different sets of S-N curves were used. Table I presents the various combinations of S-N curves and stress ranges investigated.

3. Fatigue Damage Computation

The first part of this analysis required the determination of the number of stress cycles in the various alternating stress intervals selected for this study. The number of cycles (Σy) of an alternating stress equal to or greater than a value of σ_a for a constant mean stress can be represented by

$$\Sigma y = \left[N_o P_1 e^{-\frac{\sigma_a}{\bar{A} b_1}} + N_o P_2 e^{-\frac{\sigma_a}{\bar{A} b_2}} \right] T \qquad (3)$$

where: N_o = number of zero crossings per second of response parameter

P_1 = percent of time in turbulence with scale parameter b_1

P_2 = percent of time in turbulence with scale parameter b_2

TABLE I

Aircraft, Stress Ranges, and Materials Analyzed

Aircraft	Critical Point	GW Range KIPS	Mean Stress Range, psi	Alt. Stress Range, psi	Material	Spec	KT
B-58	CP-1	80-160	3, 550-16, 000	3, 000-28, 200	Aluminum	7075-T6	4
B-58	CP-1	100-140	6, 812-13, 337	3, 000-28, 200	Aluminum	7075-T6	4
B-58	CP-1	100-140	6, 813-13, 337	2, 000-28, 200	Aluminum	7075-T6	6
B-58	CP-10	100-140	22, 176-24, 288	3, 000-28, 200	Aluminum	7075-T6	4
Hypothetical	--	--	0-72, 000	3, 000-28, 200	Steel	4130	5
F-105D	FS 509	33- 39	(-1, 000)-21, 600	2, 700-21, 600	Aluminum	7075-T6	4

$\bar{A}$ = ratio of RMS stress to RMS gust velocity

σ_a = magnitude of alternating stress, psi

T = time in seconds.

This is the well-known atmospheric turbulence model developed from Rice's[7] equations, and the model is an empirical fit of the type of curve shown in Figure 2.

The values of P and B are curve fitting parameters which were determined from empirical data for a gust environment at an altitude of 1000 feet. The term N_o is a function of the stress location on the aircraft. To simplify computations, this term was assumed to be constant for all gross weights in this analysis. The aircraft gust response factor $\bar{A}$ is a function of the aircraft flight condition and gross weight.

The values of mean stress and $\bar{A}$ for the B-58 inboard aft wheel well corner are linear functions of the gross weight. By dividing the gross weight range into the desired number of increments, the values of the mean stress and $\bar{A}$ at each of these intervals were obtained from

$$\sigma_m = -9500 + (0.163125)(\text{gross weight})$$

and

$$\bar{A} = 186 + (0.0031625)(\text{gross weight}).$$

The damage calculation was performed for the aircraft flying through the low altitude environment for T seconds at the lowest constant gross weight interval (i.e., constant mean stress). Then another T seconds of flight was accumulated at the next gross weight interval, and the damage for this flight condition was summed. This procedure was repeated for all gross weight intervals. In order to keep all computations on a directly comparable basis, each computation of fatigue damage using a different combination of mean and alternating stress interval sizes was designed to represent the same amount of flight time. For the data presented in this report, each computation represents 100,000 hours of flight time. Thus, the value of T in Equation 3 was determined by

$$T = \frac{100,000}{N_r} \tag{4}$$

where N_r is the number of mean stress intervals, and T is the time in hours at each mean stress interval. Thus, for computations using 100 mean stress intervals, a total gust spectrum representing 1000 hours of flight would be represented at each of the 100 mean stress intervals, etc.

For each analysis of fatigue damage at a given fatigue critical point for a given range of stresses, a reference damage computation was first conducted. This reference computation was designed to provide a cumulative damage value that would essentially duplicate the damage value obtained from the exact integration of Equation 2. Since the data obtained from the B-58 Service Life Monitoring Program was digitized in an 11-bit digital format, and since this level of digital resolution was thought to be more than adequate for damage computations, the reference computation was based upon using the 11-bit data directly, which in effect divided the alternating stress range into 2048 intervals. Thus, for the first analysis (one row in Table I), the reference alternating stress range was

$$\Delta\sigma_a = \frac{28,200-3000}{2048} = 12.3 \text{ psi.}$$

The mean stress range for the reference computation was arbitrarily divided into 100 intervals. Thus, for the first row of Table I, the magnitude of the reference mean stress interval was

$$\Delta\sigma_m = \frac{16,600-3550}{100} = 130.5 \text{ psi.}$$

Using these reference values of $\Delta\sigma_a$ and $\Delta\sigma_m$, the reference damage value was computed. Then in subsequent computer runs, damage computations were made for all combinations of the following numbers of mean and alternating stress intervals:

Number of Mean Stress Intervals: 100, 75, 50, 40, 35, 30, 25, 20, 15, 10, and 5;

Number of Alternating Stress Intervals: 2048, 1024, 512, 128, 100, 75, 64, 60, 50, 45, 40, 35, 32, 30, 25, 20, 15, and 10.

This procedure was repeated for each set of conditions represented by a row in Table I.

4. Comparison with a Standard

For each analysis represented by one row in Table I, a total of 198 cumulative damage computations were made (11 mean stress intervals by 18 alternating stress intervals). These damage values were then converted to damage ratios such that

$$\text{Damage Ratio} = \frac{\text{Damage}\ (\Delta\sigma_{m_i},\ \Delta\sigma_{a_j})}{\text{Damage}\ (\Delta\sigma_{m_{100}},\ \Delta\sigma_{a_{2048}})} .$$

Then, the damage ratios were plotted versus the number of alternating stress levels for a given number of mean stress intervals.

C. Results and Discussion

Figures 6, 7, 8, and 9 are plots of the damage ratio versus the number of alternating stress intervals. The ranges of the mean and alternating stress and the material analyzed are shown on the plots. These four figures are all based on a loading spectrum that would be representative of the B-58 flying at 1000 feet altitude and Mach number 0.91.

(Text continued on page 21)

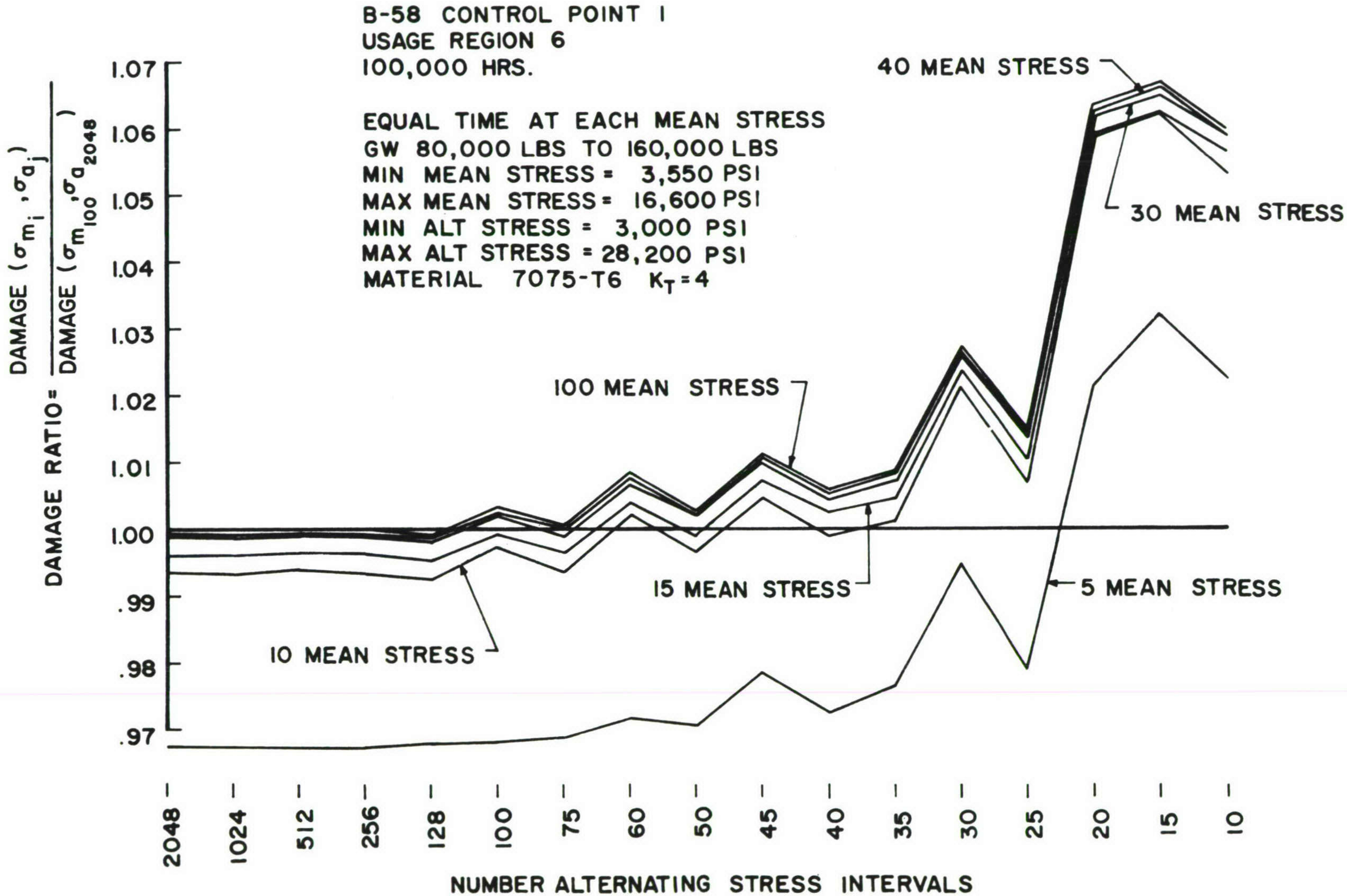

Figure 6. Damage Ratio vs Number of Alternating Stress Intervals for Various Numbers of Mean Stress Intervals; 7075-T6 Aluminum, K_T=4, Mean Stress 3550 psi to 16,600 psi

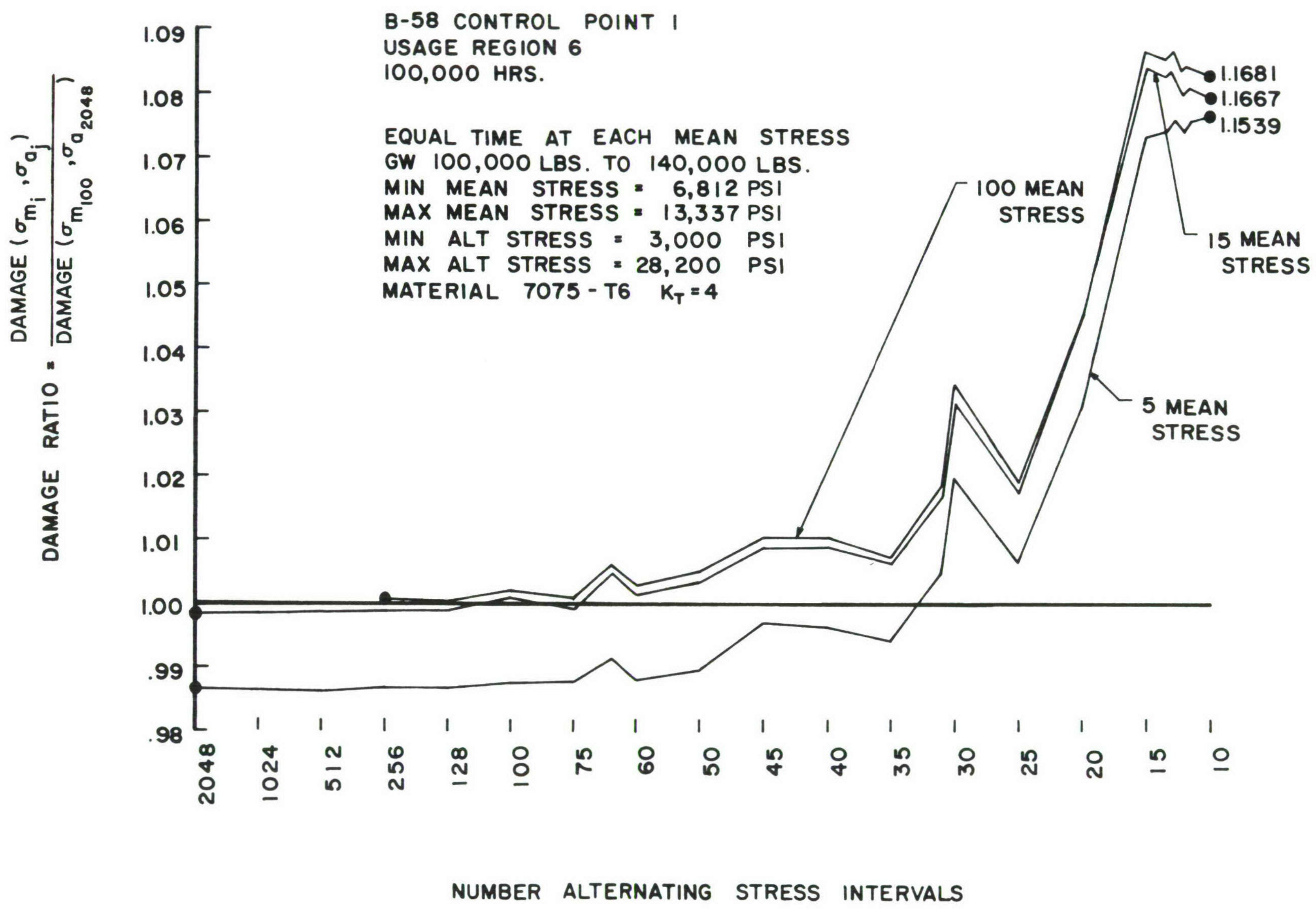

Figure 7. Damage Ratio vs Number of Alternating Stress Intervals for Various Numbers of Mean Stress Intervals; 7075-T6 Aluminum, K_T=4, Mean Stress 6812 psi to 13,337 psi

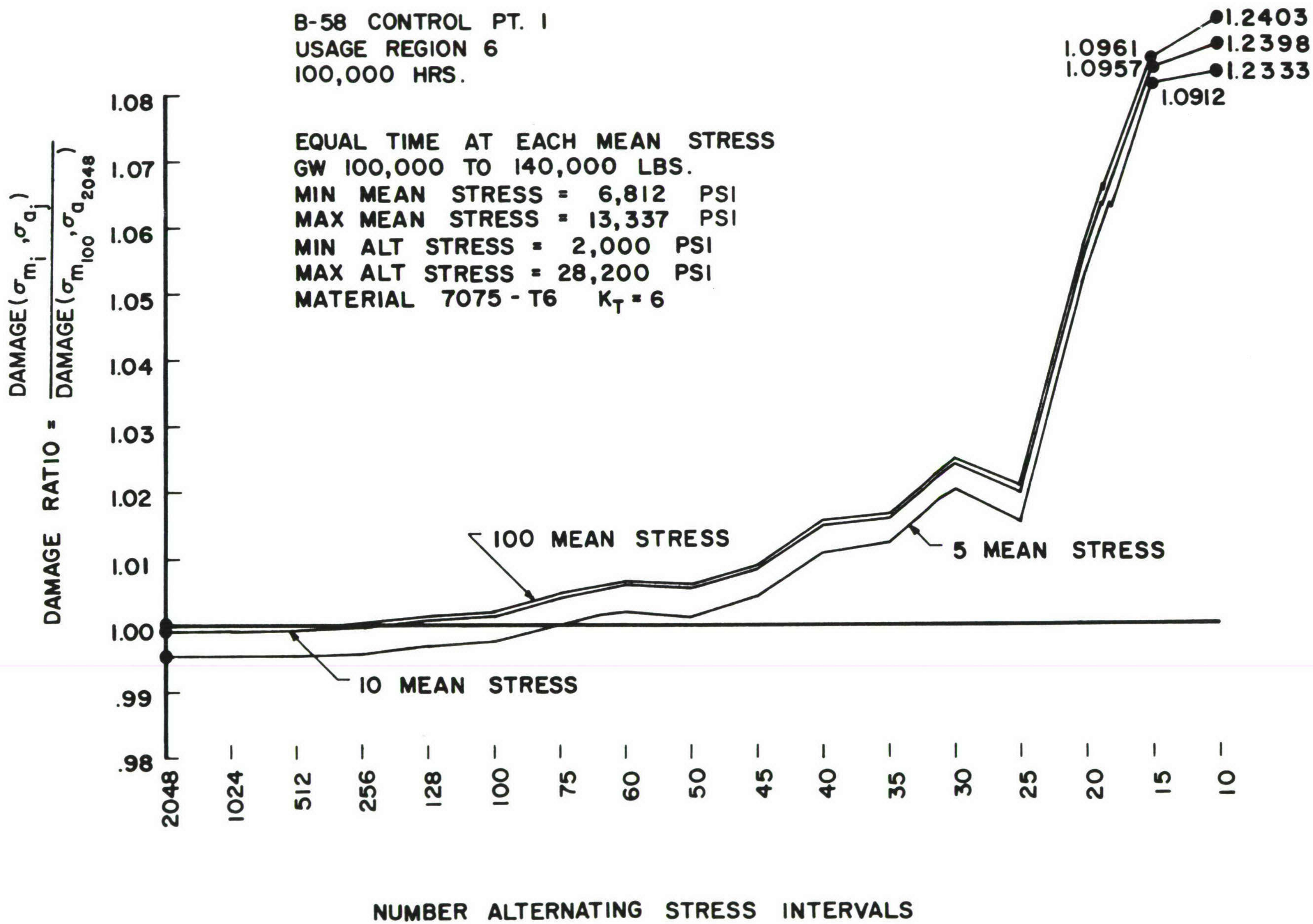

Figure 8. Damage Ratio vs Number of Alternating Stress Intervals for Various Numbers of Mean Stress Intervals; 7075-T6 Aluminum, K_T =6, Mean Stress 6812 psi to 13,337 psi

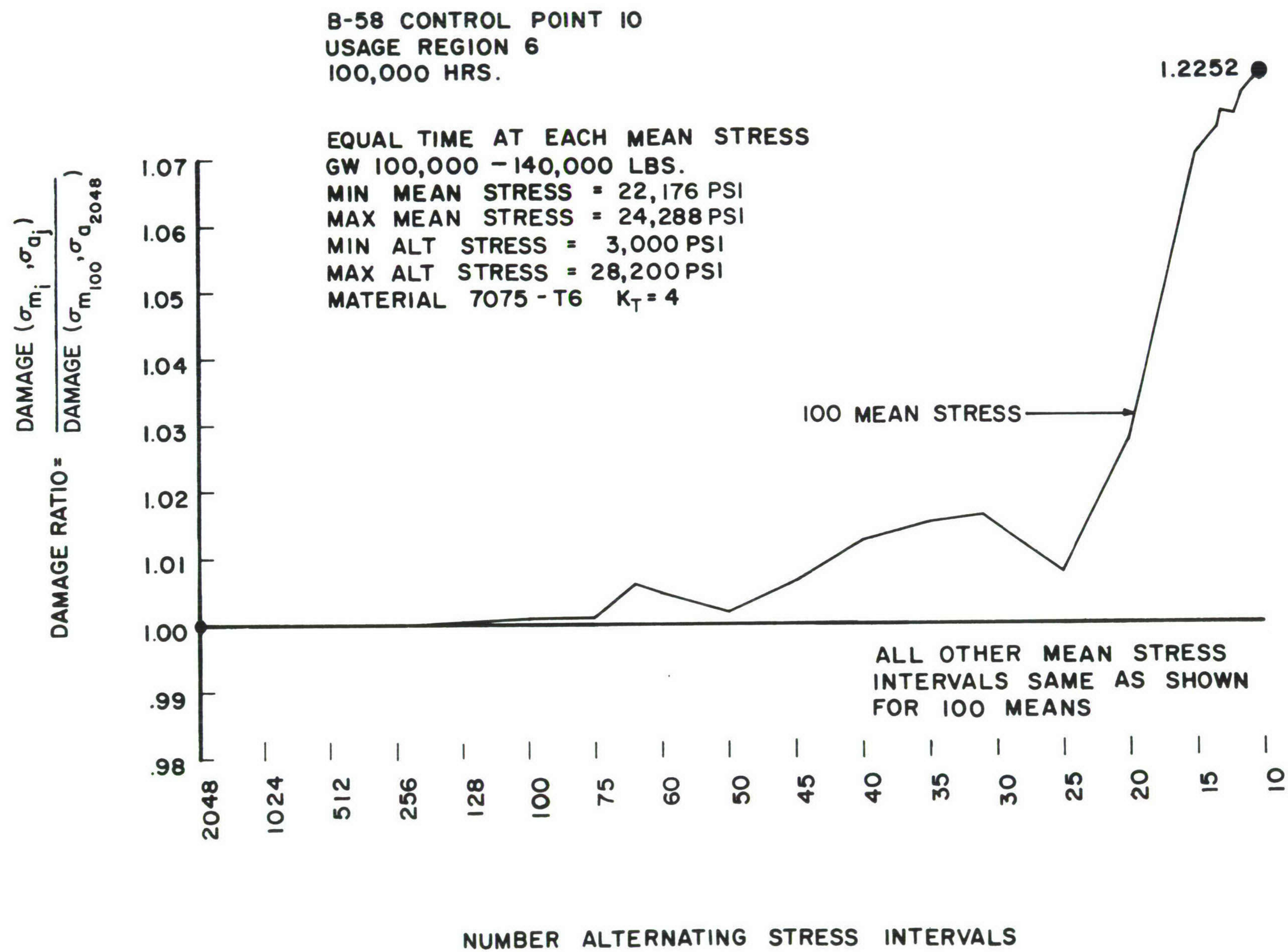

Figure 9. Damage Ratio vs Number of Alternating Stress Intervals for 100 Mean Stress Intervals; 7075-T6 Aluminum, $K_T=4$, Mean Stress 22,176 psi to 24,288 psi

Figure 10 is a plot of the damage ratio versus the number of alternating stress intervals for 4130 steel. The input data for the computations plotted in Figure 10 do not represent a real aircraft, but fictitious response parameters were used so that a large area of the S-N curves for 4130 steel would be covered. The number of stress cycles was representative of a realistic gust environment.

Figure 11 is a damage ratio plot for an F-105D maneuver spectrum. These calculations represent a typical maneuver load spectrum for fighter operations in the Southeast Asia war zone. The load factor spectrum and the curve showing the relationship between stress and load factor for the F-105D are shown, respectively, in Figure 12 and Figure 13.

The results of the fatigue analysis sensitivity study (Figures 6 through 11) indicate that, for the range of parameters investigated, the mean stress interval size has only a small effect on the magnitude of the calculated damage. Tables A-I, A-II, and A-III in Appendix A are listings of the S-N data used in the study. For the 7075-T6 material with $K_T=4$ and $K_T=6$, data were available for mean stresses of 0, 10, 20, and 30 KSI. All other values were obtained by cross plotting and interpolation.

The alternating stress interval size has a marked effect on cumulative damage computations and is dependent on the range magnitude between maximum and minimum mean stress, as is shown by the computed damage ratios for 10 alternating stress intervals on Figures 6, 7, and 9. Figure 7 shows that for a limited range of mean stress (6,800 to 13,300 psi), the damage ratio for 10 alternating stress intervals was 1.15; whereas Figure 6 shows that for a broader range of mean stresses (3,500 to 16,600 psi), the damage ratio was only 1.06. Figure 9 shows an even more dramatic effect. When the mean stress range was between 22,200 and 24,300 psi the damage ratio for 10 alternating stress intervals was 1.22. Even though Figure 10 represents the behavior of a different material (steel) than that of Figures 6, 7,

(text continued on page 26)

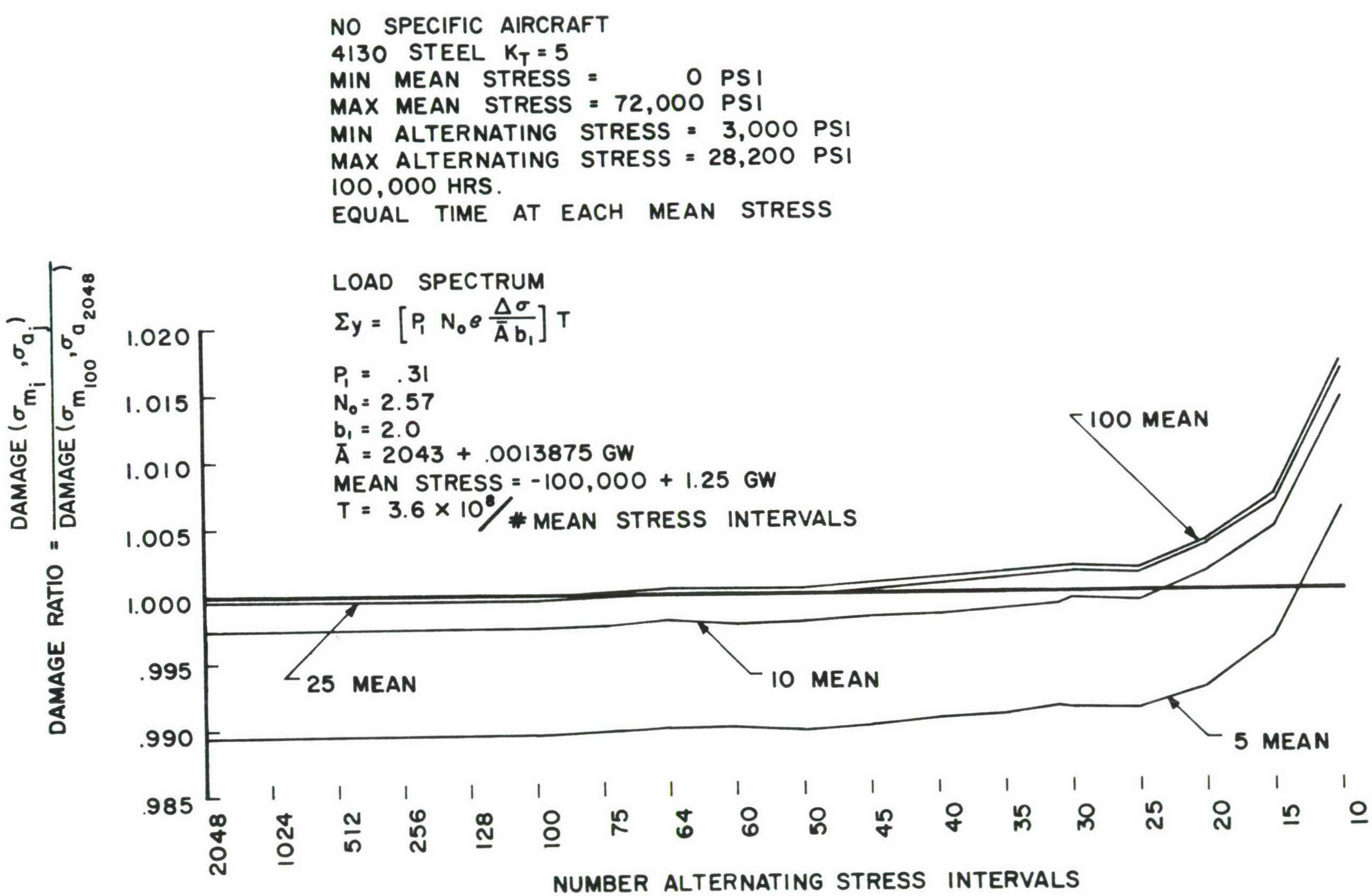

Figure 10. Damage Ratio vs Number of Alternating Stress Intervals for Various Number of Mean Stress Intervals; 4130 Steel K_T=5, Mean Stress 0 to 72,000 psi

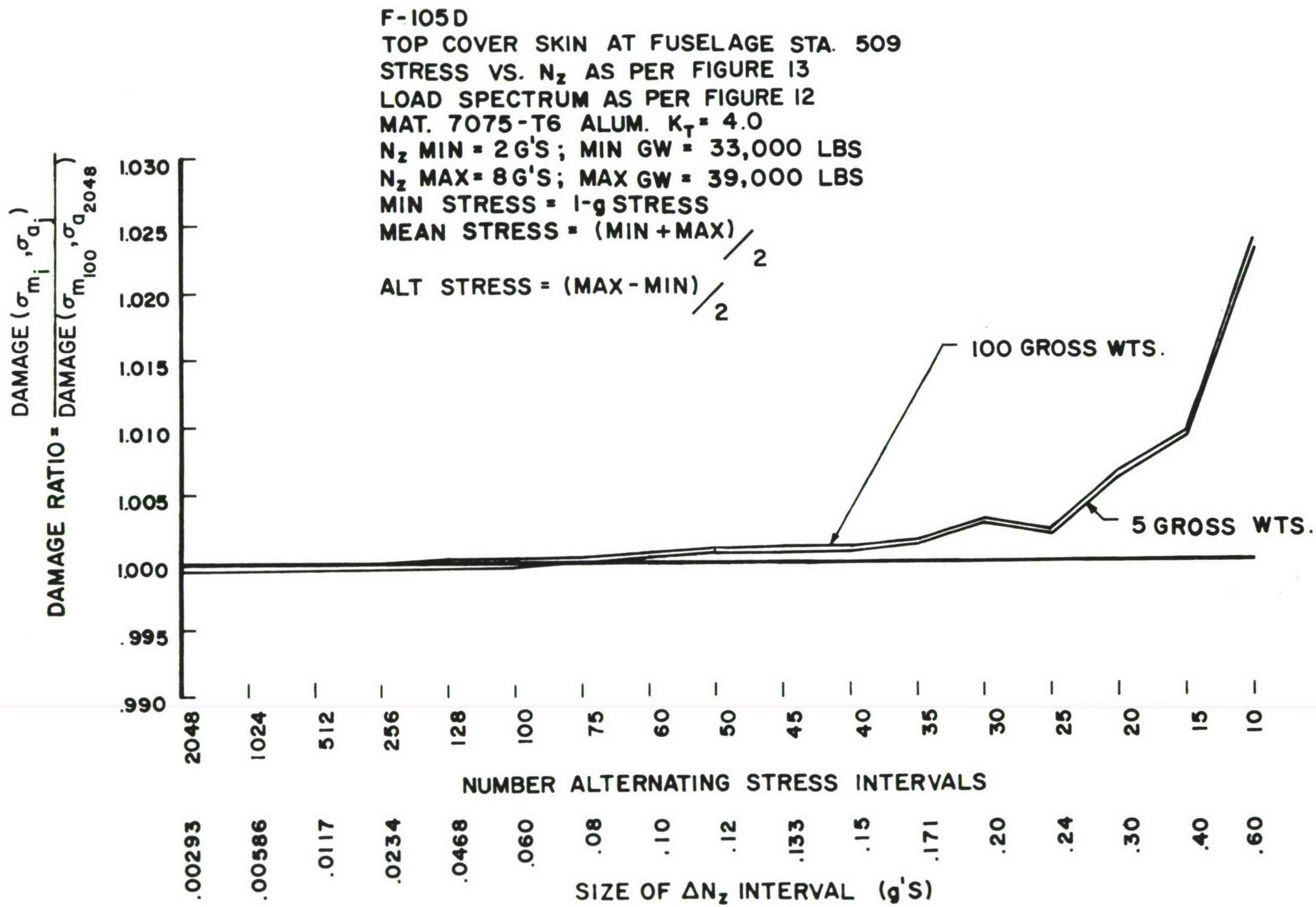

Figure 11. Damage Ratio vs Number of Alternating Stress Intervals for Various Number of Gross Weights. Maneuver Load Spectrum for Fighter-Type Aircraft

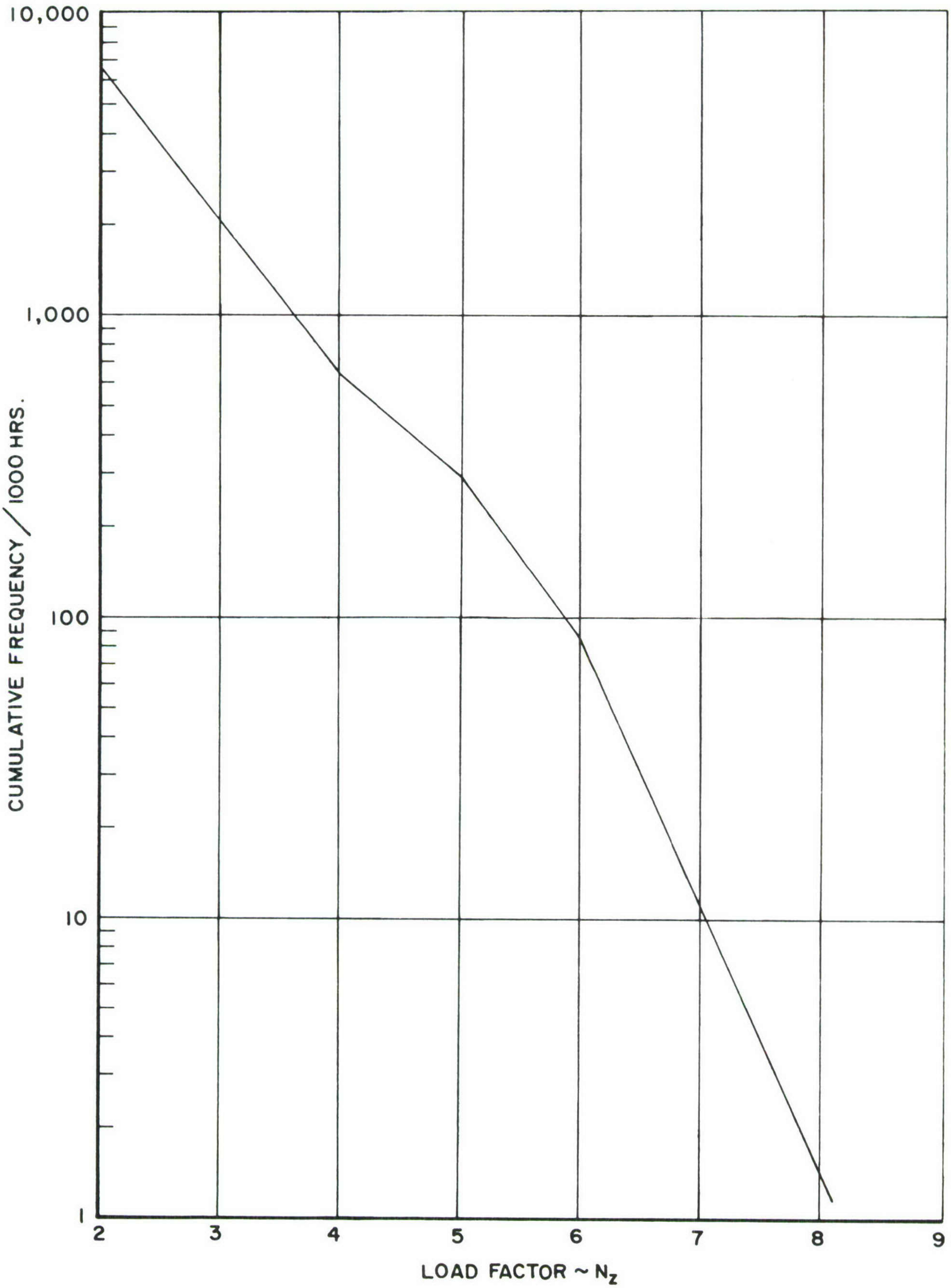

Figure 12. Cumulative Frequency of N_z for F-105D Aircraft

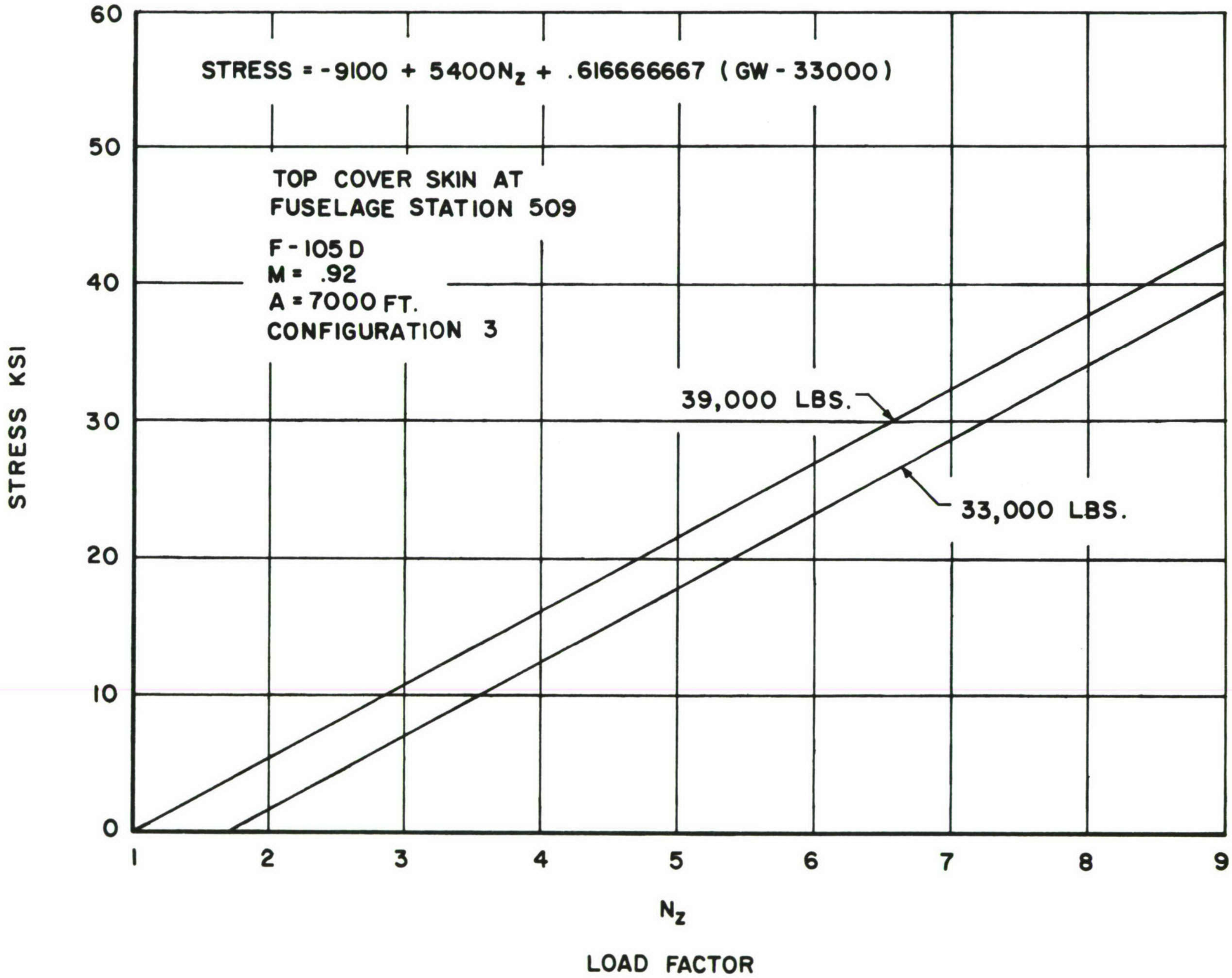

Figure 13. Stress vs Load Factor for F-105D Aircraft

and 9 (aluminum), it also shows that for a very broad range of mean stress (0 to 72,000 psi), the damage ratio for 10 alternating stress intervals was only 1.017.

After this trend had been noted, one additional set of calculations was performed in which the mean stress was held constant (25,000 psi) for the 4130 steel with K_T=5. The results of these calculations are shown in Figure 14, and they add additional verification to the trend. Table II is a summary of this comparison and clearly shows the trend of decreasing damage ratios with increasing mean stress range.

Table II

Comparison of Damage Ratios for 10 Alternating Stress Intervals for Various Ranges of Mean Stress

Mean Stress Mininum	Mean Stress Maximum	Range of Mean Stress	Damage Ratio
0	72,000	72,000	1.017
3,550	16,600	13,050	1.058
6,812	13,337	6,525	1.168
22,176	24,288	2,111	1.225
25,000	25,000	0	1.222

$$* \text{ Damage Ratio} = \frac{\text{damage at 10 alternating stress intervals}}{\text{damage at 2048 alternating stress intervals}}$$

The results of the computations shown in Figures 6 through 11 show that almost regardless of the mean stress interval size, if 30 or more intervals were used for the alternating stress, the damage ratio would be less than 1.02. Fewer numbers of alternating stress intervals caused a rapid increase

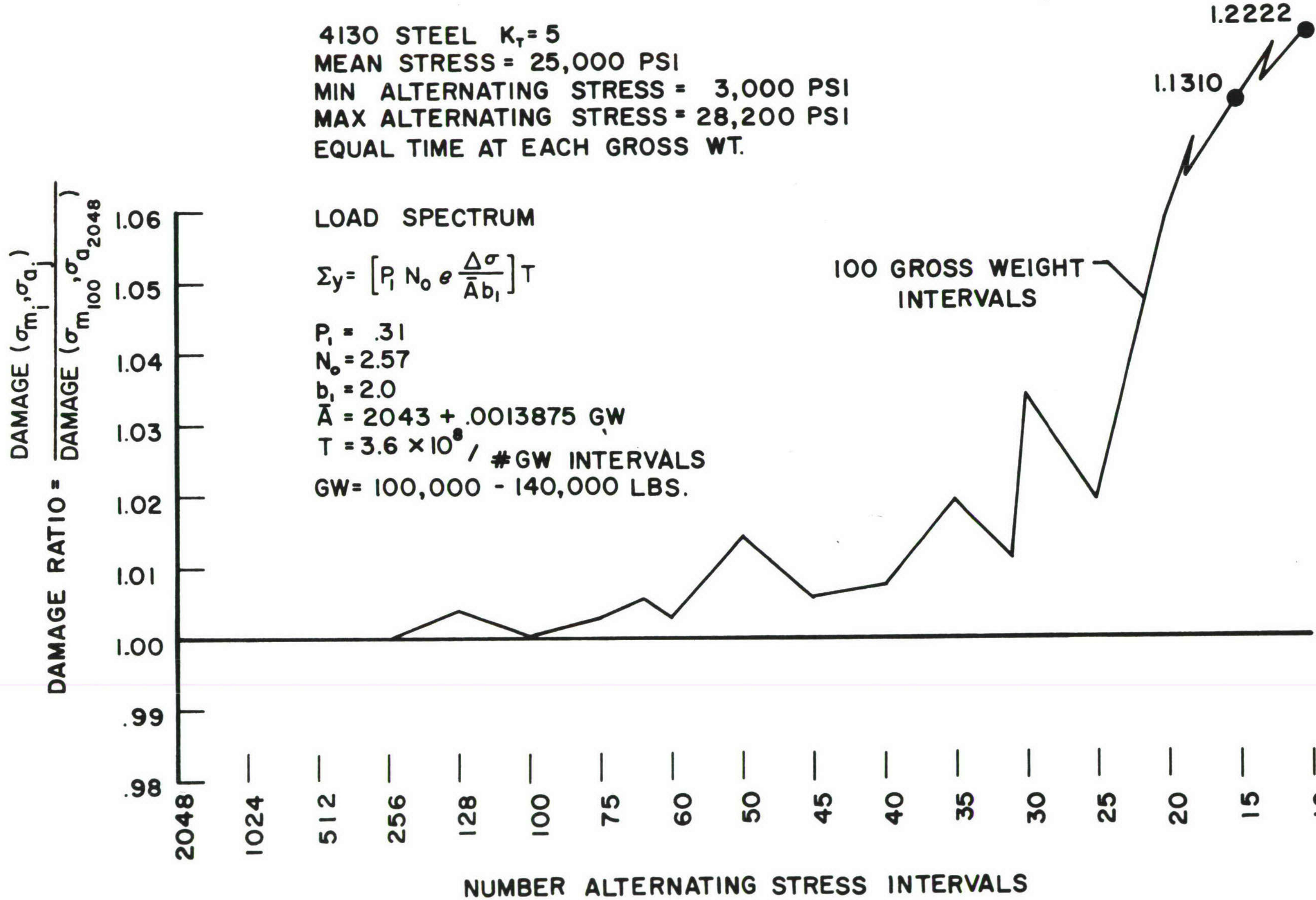

Figure 14. Damage Ratio vs Number of Alternating Stress Intervals for Constant Mean Stress, 4130 Steel, K_T=5, Mean Stress Constant at 25,000 psi

in the damage ratio. The results also show that the selection of 2048 intervals for σ_a and 100 intervals of σ_m in the reference computation for comparison was more than adequate for accurately evaluating Equation 2. This observation is substantiated by two observations: (1) the damage ratio for the 100-mean-stress curve on all of the figures was essentially 1.0 over the range from 2048 down to 256 alternating stress intervals; and (2) the addition of more than 100 mean stress intervals would have had negligible effect on the computations.

A comparison of Figures 7 and 8 shows the effect of increasing K_T on the damage ratio. With K_T=6 the lower alternating stresses cause damage, and since there are many more small amplitude cycles in a gust spectrum, more importance is shifted to the longer life end (lower σ_a magnitude) of the S-N curves. This shift in importance also caused a greater damage ratio for alternating stress intervals below 30 in number.

SECTION III

DIGITAL RESOLUTION STUDIES

The digital recorder to be developed for the ASIP will be required to measure a number of different parameters. However, the measurement of normal load factor is the most important. Consequently, this part of the study will concentrate upon the sensitivity of the normal load factor measurement accuracy to digital resolution and to the error in fatigue analysis computations resulting from using normal load factor spectra having different digital resolutions.

This study consisted of three parts: (1) the determination of the digital resolution required for N_z measurements when no correction for drift of the 1-g mean was made; (2) the determination of the digital resolution rquired for N_z measurements when corrections for the drift of the 1-g mean were made; and (3) the assessment of the digital resolution requirements for an ideal system that is free from drift.

A. Drifting Mean with No Corrections

In this study actual flight records from the B-58 Lead-the-Force program were used as the source of load factor data. This data had been recorded on FM tape, and the load factor data had been subsequently digitized at a rate of 39 samples per second into an 11-bit digital format. The resulting 11-bit digital tape was then processed by the existing B-58 EDIT program to determine the incremental load factor peaks, ΔN_z.

The data utilized for this study had instrumentation drift superimposed upon it. However, since the scope of this part of the analysis was to determine the effect of digital resolution alone, no attempt was made to correct for the drift, and the value of the 1-g mean for computing ΔN_z was the initial computed value.

The magnitude and direction of the ΔN_z and stress peaks were calculated by a series of computations. First, the digital count reading of the mean was subtracted from the digital count reading of the peak. The number of digital counts of the mean was determined by averaging the first 1000 readings recorded while the aircraft was still on the ground. Peaks were defined by the primary peak count criteria. A primary peak was defined as the maximum digitized point between two successive mean crossings by the digitized N_z time series. The incremental value of each peak in digital counts was then multiplied by the calibration factor (g/count) to obtain a ΔN_z value. The absolute value of the ΔN_z peak was then multiplied by a factor of Δstress/ΔN_z for the particular Mach-altitude and gross weight region within which the aircraft was operating. This computation yielded an alternating stress peak for each ΔN_z peak. The factor Δstress/ΔN_z was calculated using the B-58 response to a turbulent environment. Therefore, each ΔN_z peak was considered to be caused by a gust encounter.

The mean stress for each alternating stress peak was determined from the Mach-altitude and gross weight condition, and the resulting mean and alternating stresses were then used with the S-N data to determine the fatigue damage. This procedure was continued for the entire airborne portion of each flight that was analyzed, and the damage for each flight was obtained from the summation of the damage of each peak. This resulting damage fraction represented the value obtained from 11-bit data.

The 11-bit digital tape was next rewound and re-input into the computer, and a digital truncating program eliminated the 11th-bit position of all N_z data by setting the 11th bit equal to 0. In this manner, 10-bit N_z data was generated. Next, a new 1-g mean value was determined from the first 1000 readings; the data was processed again by the EDIT program; and the damage was summed yielding the damage for 10-bit data. This truncation and re-computation process was continued in order to obtain fatigue damage computations for 9, 8, 7, and 6-bit data.

For example, if an 11-bit number in binary form was

0 1 1 0 0 1 0 1 1 0 1 = 829 counts,

the 10-bit form would be

0 1 1 0 0 1 0 1 1 0 0 = 828 counts;

the 9-bit form would be

0 1 1 0 0 1 0 1 1 0 0 = 828 counts;

the 8-bit form would be

0 1 1 0 0 1 0 1 0 0 0 = 824 counts;

the 7-bit form would be

0 1 1 0 0 1 0 0 0 0 0 = 816 counts;

and the 6-bit form would be

0 1 1 0 0 1 0 0 0 0 0 = 816 counts.

The results of this digital resolution study are shown in Table III. Six complete flights were processed at each of 6 digital levels. These damages were calculated for the B-58 response parameters used with the S-N data for 7075-T6 with a K_T of 4. There was a total of 11,405 ΔN_z peaks in the 11-bit data sample.

The results shown in Table III indicate that the 11, 10, 9, and 8-bit data yielded essentially the same average fatigue damage. At a resolution of 7 bits, the damage was over-estimated by 2%, and at 6 bits the overestimate was 9%.

The reader is cautioned about relying upon the average damage differences. Within the flights chosen, damage ratios for the individual flights vary markedly from the average damage ratio. For Example, for the 6-bit data, the maximum and minimum of damage ratios were respectively, 1.22 and slightly less than 1.0. This difference in damage ratios is caused by the interaction between the actual spectrum of a given flight and the gross weight at the time the various load factors are experienced. For example, on Flight 93K, which was a low-damage flight, most of the ΔN_z peaks occurred at lower than normal

TABLE III

Fatigue Damage by Flight Record for Different Levels of Digital Resolution. Mean Position of N_z Not Corrected for Drift

Record No.	FATIGUE DAMAGE X 10^6 Bits 11	10	9	8	7	6
93K	2.7309	2.6083	2.6424	2.5016	3.1907	3.3430
76K	212.74	209.85	210.70	215.70	221.29	228.94
58L	55.766	54.552	54.250	54.985	57.459	55.461
59L	65.92	65.56	64.93	64.33	68.15	78.14
67L	511.47	506.99	504.71	503.69	512.73	546.87
97L	446.01	451.39	442.93	444.69	463.00	500.58
TOTAL	1294.6369	1290.9503	1280.1624	1285.8966	1325.8197	1413.334
RATIO *	1.0	.9972	.9888	.9932	1.0241	1.0917
RATIO **	1.1596	1.1563	1.1466	1.1518	1.1875	1.2659

*Ratio was calculated by dividing the above total damage by total damage for 11-bit data with constant mean. This is the error due to resolution alone.

**Ratio was calculated by dividing above total damage by total damage for 11-bit data with mean position corrected for drift, i.e., divide by 1116.47×10^{-6}. This is the combined error due to drift plus resolution error (See Table IV) gross weights, and therefore these peaks caused lower than normal alternating stresses. However, on Flight 97L, which was a high-damage flight, the ΔN_z peaks having the same magnitude as those on Flight 93K caused higher alternating stresses because the peaks occurred at higher gross weights. It is well known that because of the highly non-linear shape of the S-N curve, a given incremental change in a low-magnitude alternating stress causes a relatively large change in the number of cycles to failure (N_i and hence in the cumulative damage D) than the same incremental change would cause at higher-magnitude alternating stress levels. Therefore, a given digital resolution error in ΔN_z (and thus in the resulting alternating stress) would result in a larger damage error for a light-weight aircraft than for a heavy-weight aircraft. Thus, when a ΔN_z spectrum is converted into stress spectrum which is concentrated toward the low-stress-long-life end of the S-N curve, more ΔN_z spectrum accuracy is required than if a high-magnitude stress spectrum were realized.

The reader can ascertain from Table III that the variation in the damage ratio decreases from flight by flight as the number of digital bits increases. For the 7-bit data sample, the variation is from 1.17 to 1.00; for 8-bit data the variation is from 0.92 to 1.01; and for 9-bit data the variation is from 0.97 to 0.99. Thus, the fatigue damage computation would be essentially insensitive to 9-bit data, and 8-bit data resolution probably would be the minimum acceptable level for a general purpose recorder.

B. Drifting Mean with Corrections

The procedure for this study was the same as that previously described in Section IIIA, except that the data were corrected by removing drift effects caused by the instrumentation system installed in the B-58 Lead-the-Force fleet. In the solution of this problem, the mean (1-g trim) position was determined as before by computing the average of the first 1000 readings (while the aircraft was still on the ground). For times after the occurrence of the first 1000 readings, the mean position was determined by the following equation which is a recursive filter:

$$\text{Mean}_{t_2} = \text{Mean}_{t_1} - (\text{Mean}_{t_1} - DP_{t_2})(0.0001)$$

where DP is the digital value of the N_z data point at time t_2, and $t_2 > t_1$.

In order to eliminate the positive biasing effect on the mean caused by maneuvers, only data points having values within limiting bands on each side of the mean at time t_1 were used to compute the new value of the mean at time t_2. The magnitude of this limiting band was ±0.05g for the 11, 10, 9, 8, and 7-bit data. Inasmuch as the 6-bit digital system used for this study could not resolve a ΔN_z value as small as 0.05g (and hence was unable to correct for mean drift because no points fell within ±0.05g), the limiting band was increased to ±0.15g.

After incorporating the mean shift correction, the processing of the flights for this study was the same as that described for the non-drifting mean analysis. The results of this study are shown in Table IV, which summarizes the total damages obtained for each of the same six flights.

Table V is a set of cumulative frequency distributions for ΔN_z data that would be used to plot a curve similar to Figure 2. There is one distribution for each of the six digital resolutions studied.

One's first observation from studying the data in Table IV is that there appears to be very little difference in the average damage ratios of the 11-bit data and the 6-bit data. However, the reader must keep in mind that the average damage ratios were computed from a small sample of six flights that are not necessarily representative of a complete gust spectrum and operational regime of the aircraft. Again, looking at the individual flight damage ratios as was done in the analysis of Section II A, one can determine that there is variation of damage ratios from 0.81 to 1.08 at the 6-bit level, whereas the damage ratio variation at the 8-bit level is 0.98 to 1.02. Thus

TABLE IV

Fatigue Damage by Flight Record for Different Levels of Digital Resolution. Mean Position of N_z Corrected for Drift

FATIGUE DAMAGE X 10^6						
Record No.	Bits					
	11	10	9	8	7	6
93K	1.0240	1.0225	.9616	1.0456	.93863	.83461
76K	170.42	169.03	169.56	168.00	165.94	178.46
58L	48.798	47.981	48.278	48.777	50.676	49.875
59L	46.82	46.78	46.84	45.59	47.49	38.18
67L	443.13	443.37	439.09	432.19	435.17	451.44
97L	406.28	404.49	404.92	404.59	413.56	438.58
TOTAL	1116.47	1112.67	1109.65	1100.19	1113.77	1157.37
RATIO	1	.9966	.9934	.9854	.9975	1.0366

TABLE V

Cumulative Occurrences of ΔN_z for Various Levels of Digital Resolution

ΔN_z Band	BITS					
	11	10	9	8	7	6
.10-.15	9892	9909	9894	10100	9400	11094
.15-.20	4392	4394	4405	4304	4983	4717
.20-.25	2156	2146	2164	2093	2111	2099
.25-.30	1120	1121	1117	1110	1173	1084
.30-.35	587	594	593	603	613	588
.35-.40	304	309	304	311	283	337
.40-.45	158	161	161	154	177	163
.45-.50	70	71	71	66	71	72
.50-.55	31	32	32	31	34	35
.55-.60	17	17	18	18	20	22
.60-.65	9	9	9	9	10	8
.65-.70	5	5	5	5	7	5
.70-.75	2	2	2	2	2	2
.75-.80	1	1	1	1		

Entries are the sum of all ΔN_z regardless of whether the peak was + or - gust or maneuver. The data sample included all peaks on flights 93K, 76K, 58L, 59L, 67L, and 97L independent of W-H-A.

again, an 8-bit resolution would appear to be the minimum acceptable level.

The effect of not correcting for the drift of the N_z mean line can be determined by looking at the two sets of damage ratios presented in Table III, and the differences in these sets is explained at the bottom of the table. This information indicates that for drift amounting to 2% of full scale (which was experienced on the B-58 program and is normal for the strain-gage type accelerometers currently in use on other flight loads programs), an average error of 16% and 26% caused by drift plus digital resolution would be expected in 11-bit and 6-bit data, respectively. Since the results of Table IV indicate the damage ratio caused by resolution error alone, it can be seen that even the minimal amount of drift experienced by the B-58 system can cause appreciable error in the data if compensating corrections are not made.

It is surprising to note from an examination of Table V that such a marked difference in the cumulative spectra occurred as the number of digital bits was decreased from 11 to 6. Differences between the 11-bit and 6-bit distributions were relatively small up to the 0.20-0.25 class interval, but for smaller ΔN_z levels the differences were larger. These differences in the number of peaks can be attributed to the following three interacting phenomena which may or may not compensate for each other: (1) the resolution error between 11-bit and 6-bit data affects the magnitude of the N_z value (see Table V) and causes data points to shift from one ΔN_z band to another depending upon the relative positions of the class interval boundaries and the actual magnitude of the set of data points; (2) the accuracy of determining the N_z mean position and correcting for mean drift depends upon the digital resolution ($\Delta N_z = N_z$-Mean), and hence affects the value of ΔN_z; and (3) the primary peak editing criteria causes points either to be added or subtracted from the spectrum because of mean shifts resulting from digital resolution errors.

The first two reasons for the variation in the number of peaks as a function of digital resolution are self-explanatory, but the third reason needs more clarification. As was previously stated, a primary peak is defined as the digital point having the largest absolute value between two successive crossings of the N_z mean level by the digital time series obtained from the N_z measurement. By referring to Figure 15, one can see the effect that the application of the editing criteria combined with a shift in the mean line will have on the definition of primary N_z peaks. Not only will the number of peaks be different for each mean line position, but also the magnitude of each peak will change.

The variation in ΔN_z peaks from one flight to the next is not shown in Table V, but the results are comparable to the damage ratios in Tables III and IV; i.e., the flight by flight variation is greater than the average variation. As in the damage tables, one must conclude that for consistently good data from flight to flight, a digital resolution at least equal to 8 digital bits is required.

One might ask the question: why is it that the total ΔN_z distributions appear to vary so markedly from 11-bit data to 6-bit data, and yet the average damage ratio errors in Table IV are significantly smaller? The answer lies in the damage density curve of Figure 5. For the B-58 critical points selected, the threshold of damage, which is about 0.3g, varies with Mach number, altitude, and gross weight. From Table V it can be seen that the differences in the spectra above the 0.3g level are small. However, on individual flights, an unusually different spectrum shape might change the damage density curve for that flight. For example, Flight 93K had very many low-magnitude gust cycles and several high-magnitude cycles. Since the gross weight was relatively low, the stresses were low. Because of these conditions the alternating stresses were concentrated in the area of the S-N curve where 6-bit resolution errors cause large variations in the

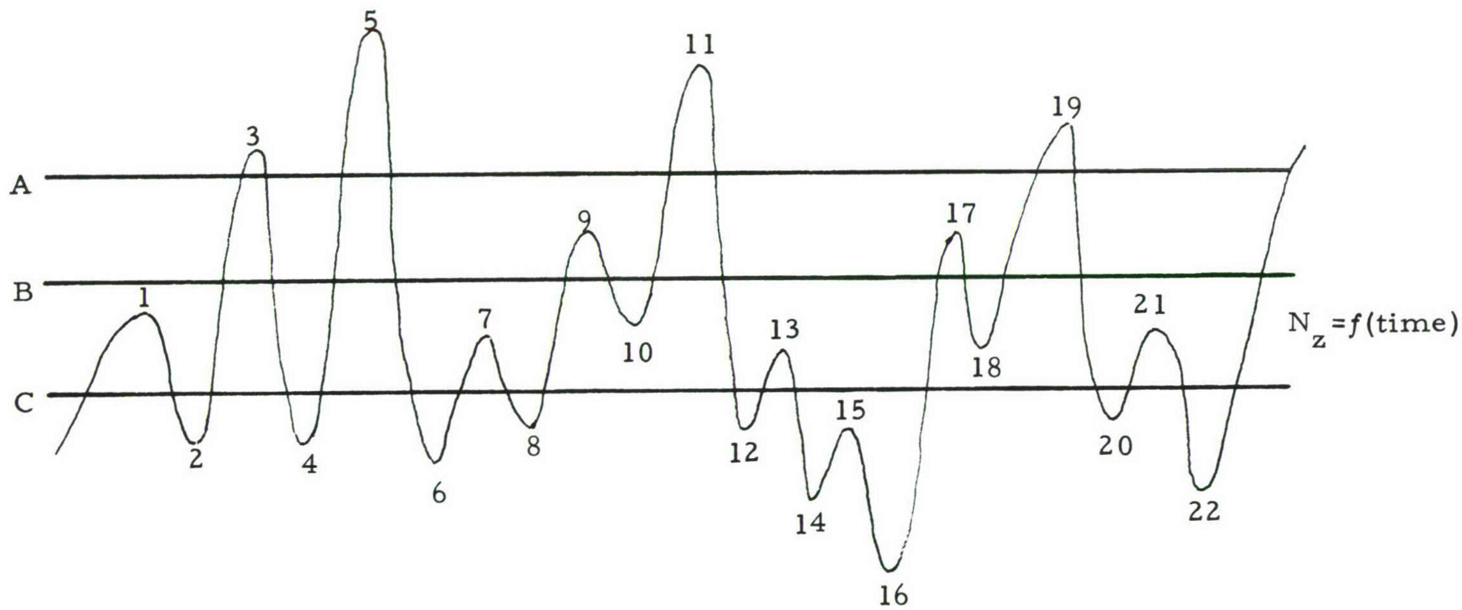

MEAN LINE	PRIMARY PEAKS															
Resolution A	3	4	5	6	11	16	19	22								
Resolution B	3	4	5	6	9	10	11	16	17	18	19	22				
Resolution C	1	2	3	4	5	6	7	8	11	12	13	16	19	20	21	22

Figure 15. Effect of Editing Criteria on Variation in Number of Primary ΔN_z Peaks Counted for Mean Lines Determined by Data Having Various Digital Resolution Levels

number of cycles to failure, and thus the difference in damage between 11-bit and 6-bit data was large.

The significance of these errors in damage computations and ΔN_z spectra to the ASIP recorder is that the Air Force wants to purchase a general purpose recorder capable of fulfilling recording needs for all types of aircraft. Thus, for general purpose work, an 8-bit resolution seems to be justified.

Further justification of an 8-bit instrument is that the recording oscillograph systems currently being used for flight loads work can be used to provide 9-bit data. The oscillograph has demonstrated its ability to record useful data from practically every type of transducer in use for flight test work, and hence the digital ASIP recorder should have a similar capability.

Another requirement of the ASIP recorder is governed by one of the basic ASIP objectives: the development of design criteria for future aircraft. The intent will be to record gust and maneuver spectra from currently operating aircraft and use the data to design future aircraft. Thus, even though a ΔN_z spectrum derived from 6-bit data, as shown in Table V, might be adequate for the B-58 aircraft and possibly for current high load factor fighter aircraft, the damage density curve of a larger, more flexible aircraft such as the C-5 and the Boeing 747 might reflect a high sensitivity to low magnitude stresses. This condition actually has been observed in heavy gross weight conditions of the B-52, where an appreciable fraction of total fatigue damage occurred at incremental load factor levels of 0.10g. Thus, care should be taken to assure that the low magnitude portion of load factor spectra is reasonably accurate if the data are to be used for design criteria.

C. Ideal System

The last digital resolution study was conducted for an ideal instrumentation system. This system would be one which would be composed of transducer, transmission line, signal conditioning, and recorder components that would provide completely drift-free operation. This system sensitivity in terms of g's per count, for example, also would remain linear and constant with time. Finally, the sensitivity and reference levels would have to be the same in all systems installed in ASIP aircraft.

With a system such as this, it would be possible to select the class interval boundaries of a discrete ΔN_z spectrum such that they coincide exactly with the digital levels of the recorder. If such a system were designed, all points falling within a given digital interval would automatically fall within a given class interval of ΔN_z because the digital and ΔN_z class interval boundaries would exactly coincide. In this way, the accuracy of the resulting spectrum would not be dependent on the digital resolution. All that would be required would be to provide enough digital intervals to represent the shape of the load factor spectrum accurately. (Probably 4 or 5-bit data would suffice.)

To illustrate the way in which the coincidence (or lack of it) in digital levels and ΔN_z spectral boundaries affects cumulative fatigue damage computations, two sets of computations were made using 11, 10, 9, 8, 7, and 6-bit data for each set. The first set of computations aligned the ΔN_z class interval boundaries with the digital boundaries, and the second set of computations established ΔN_z class interval boundaries at 0.05 g intervals, which did not coincide with the digital boundaries. The spectrum, aircraft parameters, and S-N data used for these computations are listed in Table VI. The results of this study are listed in Table VII and Table VIII.

The results in Table VII pertain to the first set of computation in which the digital and ΔN_z boundaries coincided. One can see that as the number of digital bits decreases, the damage generally increases but only slightly. This error is the result of using class intervals that are too wide for a precise integration of Equation 2. The error for 6-bit data is not very high, as might be expected, because a 6-bit system would divide the load factor spectrum

(Text continued on page 45)

TABLE VI

Parameters Used for Calculations Presented in Tables VII and VIII

$$\Sigma n = T\left[P_1 N_o e^{-\frac{\Delta N}{\bar{A} b_1}} + P_2\, N_o\, e^{-\frac{\Delta N}{\bar{A} b_2}}\right]$$

where Σn = cumulative cycles of ΔN_z

T = Time

N_o = Number of zero crossings with positive slope

$\bar{A}_{cg}$ = Ratio of RMS load factor response to RMS gust velocity

$b_{1,2}$ = Scale parameter of gust distribution

$P_{1,2}$ = Percent of time in turbulence

$$\text{Alternating stress} = (\Delta N)\left(\frac{\bar{A}_s}{\bar{A}_{cg}}\right)$$

where $\bar{A}_s$ = ratio of RMS stress to RMS gust velocity

Mean stress = 1-g trim stress

The following values were used:

USAGE REGION 1	USAGE REGION 4	USAGE REGION 8
$T = 3.6\times10^6$	$T = 3.6\times10^6$	$T = 3.6\times10^6$
$P_1 = .31$	$P_1 = .36$	$P_1 = .03$
$P_2 = 0$	$P_2 = 0$	$P_2 = .0012$
$b_1 = 2.00$	$b_1 = 2.69$	$b_1 = 2.21$
$b_2 = 0$	$b_2 = 0$	$b_2 = 4.62$
$N_o = 1.96$	$N_o = 2.22$	$N_o = 1.62$
$\bar{A}_{cg} = .0608-.1825\times10^{-6}$ (GW)	$\bar{A}_{cg} = .0593-.1750\times10^{-6}$ (GW)	$\bar{A}_{cg} = .0324-.1112\times10^{-6}$ (GW)
$\bar{A}_s = 57+.0008625$(GW)	$\bar{A}_s = 49+.003025$(GW)	$\bar{A}_s = 50+.000975$(GW)
1-g stress = 400+.060 (GW)	1-g stress = -900+.0675 (GW)	1-g stress = -2900+.10625 (GW)

TABLE VII

Damage Rates vs Flight Regime for Various Levels of Digital Resolution. Ideal System with Digital Levels and ΔN_z Boundaries Coinciding

Damage/1000 hours for Various Usage Regions, Gross Weights, and Bits of Data
No Drift Ideal System

Usage Region	Gross Weight (kips)	Damage/1000 Hr.					
		11 Bits	10 Bits	9 Bits	8 Bits	7 Bits	6 Bits
1	80	7.4675×10^{-8}	7.4677×10^{-8}	7.4668×10^{-8}	7.4912×10^{-8}	7.4504×10^{-8}	7.8356×10^{-8}
	90	9.1667×10^{-7}	9.1662×10^{-7}	9.1661×10^{-7}	9.1631×10^{-7}	9.2953×10^{-7}	9.1182×10^{-7}
	100	5.7179×10^{-6}	5.7166×10^{-6}	5.7124×10^{-6}	5.7343×10^{-6}	5.7430×10^{-6}	5.8485×10^{-6}
	110	2.3491×10^{-5}	2.3544×10^{-5}	2.3536×10^{-5}	2.3458×10^{-5}	2.3469×10^{-5}	2.4138×10^{-5}
	120	7.3328×10^{-5}	7.3333×10^{-5}	7.3355×10^{-5}	7.3436×10^{-5}	7.3762×10^{-5}	7.5948×10^{-5}
	130	1.8472×10^{-4}	1.8450×10^{-4}	1.8455×10^{-4}	1.8492×10^{-4}	1.8538×10^{-4}	1.8885×10^{-4}
	140	3.9049×10^{-4}	3.9049×10^{-4}	3.8862×10^{-4}	3.8840×10^{-4}	3.9199×10^{-4}	4.0039×10^{-4}
	150	7.1495×10^{-4}	7.1495×10^{-4}	7.1093×10^{-4}	7.2056×10^{-4}	7.1626×10^{-4}	7.3020×10^{-4}
	160	1.1681×10^{-3}	1.1688×10^{-3}	1.1680×10^{-3}	1.1673×10^{-3}	1.1739×10^{-3}	1.2259×10^{-3}
4	80	6.0023×10^{-4}	6.0025×10^{-4}	6.0029×10^{-4}	6.0025×10^{-4}	5.9788×10^{-4}	6.1198×10^{-4}
	90	2.7614×10^{-3}	2.7615×10^{-3}	2.7619×10^{-3}	2.7646×10^{-3}	2.7693×10^{-3}	2.7994×10^{-4}
	100	8.5020×10^{-3}	8.5028×10^{-3}	8.5054×10^{-3}	8.5096×10^{-3}	8.5170×10^{-3}	8.6252×10^{-3}
	110	2.0283×10^{-2}	2.0282×10^{-2}	2.0282×10^{-2}	2.0293×10^{-2}	2.0347×10^{-2}	2.0516×10^{-2}
	120	4.0465×10^{-2}	4.0468×10^{-2}	4.0472×10^{-2}	4.0612×10^{-2}	4.0525×10^{-2}	4.0797×10^{-2}
	130	7.0966×10^{-2}	7.0964×10^{-2}	7.0984×10^{-2}	7.1022×10^{-2}	7.1258×10^{-2}	7.1651×10^{-2}
	140	1.1212×10^{-1}	1.1205×10^{-1}	1.1206×10^{-1}	1.1212×10^{-1}	1.1331×10^{-1}	1.1374×10^{-1}
	150	1.6270×10^{-1}	1.6255×10^{-1}	1.6293×10^{-1}	1.6245×10^{-1}	1.6394×10^{-1}	1.6465×10^{-1}
	160	2.1988×10^{-1}	2.1991×10^{-1}	2.2039×10^{-1}	2.2005×10^{-1}	2.2121×10^{-1}	2.2577×10^{-1}
8	80	1.2261×10^{-7}	1.2660×10^{-7}	1.2661×10^{-7}	1.2661×10^{-7}	1.2759×10^{-7}	1.2927×10^{-7}
	90	8.7823×10^{-7}	8.7822×10^{-7}	8.7832×10^{-7}	8.7946×10^{-7}	8.7982×10^{-7}	9.0370×10^{-7}
	100	3.8181×10^{-6}	3.8187×10^{-6}	3.8194×10^{-6}	3.8225×10^{-6}	3.8340×10^{-6}	3.8561×10^{-6}
	110	1.2131×10^{-5}	1.2152×10^{-5}	1.2112×10^{-5}	1.2115×10^{-5}	1.2156×10^{-5}	1.2734×10^{-5}
	120	3.0215×10^{-5}	3.0218×10^{-5}	3.0218×10^{-5}	3.0252×10^{-5}	3.0831×10^{-5}	3.0764×10^{-5}
	130	6.2817×10^{-5}	6.2838×10^{-5}	6.2833×10^{-5}	6.2891×10^{-5}	6.2778×10^{-5}	6.4544×10^{-5}
	140	1.1229×10^{-4}	1.1232×10^{-4}	1.1218×10^{-4}	1.1254×10^{-4}	1.1387×10^{-4}	1.1689×10^{-4}
	150	1.7941×10^{-4}	1.7946×10^{-4}	1.7945×10^{-4}	1.7988×10^{-4}	1.8067×10^{-4}	1.8942×10^{-4}
	160	2.5978×10^{-4}	2.6073×10^{-4}	2.6079×10^{-4}	2.6022×10^{-4}	2.6163×10^{-4}	2.7027×10^{-4}

TABLE VIII

Damage Rates vs Flight Regime for Various Levels of Digital Resolution. Ideal System with Data Blocked in 0.05 g ΔN_z Intervals

Usage Region	Gross Weight (kips)	Damage/1000 Hr.					
		11 Bits	10 Bits	9 Bits	8 Bits	7 Bits	6 Bits
1	80	7.5956×10^{-8}	7.5145×10^{-8}	7.3137×10^{-8}	7.0483×10^{-8}	6.4781×10^{-8}	5.5112×10^{-8}
	90	9.0457×10^{-7}	8.9497×10^{-7}	8.8073×10^{-7}	8.3358×10^{-7}	7.7432×10^{-7}	7.0664×10^{-7}
	100	5.7152×10^{-6}	5.6651×10^{-6}	5.5555×10^{-6}	5.3025×10^{-6}	4.7817×10^{-6}	3.9750×10^{-6}
	110	2.3974×10^{-5}	2.3627×10^{-5}	2.3147×10^{-5}	2.2216×10^{-5}	2.0549×10^{-5}	1.8075×10^{-5}
	120	7.3242×10^{-5}	7.2263×10^{-5}	7.0068×10^{-5}	6.6712×10^{-5}	6.2826×10^{-5}	5.0709×10^{-5}
	130	1.8713×10^{-4}	1.8557×10^{-4}	1.7933×10^{-4}	1.7420×10^{-4}	1.5895×10^{-4}	1.3250×10^{-4}
	140	3.9210×10^{-4}	3.8878×10^{-4}	3.7727×10^{-4}	3.5580×10^{-4}	3.2553×10^{-4}	2.6689×10^{-4}
	150	7.0676×10^{-4}	6.9624×10^{-4}	6.7657×10^{-4}	6.3932×10^{-4}	5.5740×10^{-4}	4.2631×10^{-4}
	160	1.2028×10^{-3}	1.1761×10^{-3}	1.1441×10^{-3}	1.0908×10^{-3}	0.94301×10^{-3}	6.8834×10^{-4}
4	80	6.0926×10^{-4}	6.0584×10^{-4}	5.9820×10^{-4}	5.7453×10^{-4}	5.3868×10^{-4}	4.8519×10^{-4}
	90	2.7467×10^{-3}	2.7209×10^{-3}	2.6755×10^{-3}	2.5836×10^{-3}	2.4340×10^{-3}	2.1820×10^{-3}
	100	8.4765×10^{-3}	8.4021×10^{-3}	8.2427×10^{-3}	8.0316×10^{-3}	7.6104×10^{-3}	6.6375×10^{-3}
	110	2.0216×10^{-2}	2.0091×10^{-2}	1.9697×10^{-2}	1.9092×10^{-2}	1.8072×10^{-2}	1.5537×10^{-2}
	120	4.0339×10^{-2}	4.0018×10^{-2}	3.9248×10^{-2}	3.7946×10^{-2}	3.5211×10^{-2}	3.0293×10^{-2}
	130	7.1287×10^{-2}	7.0389×10^{-2}	6.9040×10^{-2}	6.6511×10^{-2}	6.0885×10^{-2}	5.0537×10^{-2}
	140	1.1193×10^{-1}	1.1032×10^{-1}	1.0843×10^{-1}	1.0504×10^{-1}	0.94965×10^{-3}	7.8731×10^{-2}
	150	1.6232×10^{-1}	1.6017×10^{-1}	1.5738×10^{-1}	1.5281×10^{-1}	1.3775×10^{-1}	1.1885×10^{-1}
	160	2.2154×10^{-1}	2.1919×10^{-1}	2.1518×10^{-1}	2.0873×10^{-1}	1.8761×10^{-1}	1.6870×10^{-1}
8	80	1.2641×10^{-7}	1.2534×10^{-7}	1.2357×10^{-7}	1.1916×10^{-7}	1.0969×10^{-7}	0.96506×10^{-7}
	90	8.8727×10^{-7}	8.7917×10^{-7}	8.6572×10^{-7}	8.3331×10^{-7}	7.7851×10^{-7}	6.9607×10^{-7}
	100	3.8272×10^{-6}	3.7865×10^{-6}	3.7071×10^{-6}	3.5781×10^{-6}	3.3981×10^{-6}	2.8836×10^{-6}
	110	1.1959×10^{-5}	1.1880×10^{-5}	1.1619×10^{-5}	1.1240×10^{-5}	1.0598×10^{-5}	0.91554×10^{-5}
	120	3.0483×10^{-5}	3.0166×10^{-5}	2.9443×10^{-5}	2.8202×10^{-5}	2.5727×10^{-5}	2.0970×10^{-5}
	130	6.3746×10^{-5}	6.2661×10^{-5}	6.1308×10^{-5}	5.9046×10^{-5}	5.2866×10^{-5}	4.1548×10^{-5}
	140	1.1262×10^{-4}	1.1040×10^{-4}	1.0814×10^{-4}	1.0368×10^{-4}	9.1779×10^{-5}	0.74339×10^{-4}
	150	1.8125×10^{-4}	1.7877×10^{-4}	1.7593×10^{-4}	1.6977×10^{-4}	1.4536×10^{-4}	1.3178×10^{-4}
	160	2.6616×10^{-4}	2.6435×10^{-4}	2.5714×10^{-4}	2.5042×10^{-4}	2.2162×10^{-4}	2.0515×10^{-4}

(and hence the alternating stress spectrum) into 64 intervals. As shown in Figures 6 and 9, the integration error is negligible when more than 30 alternating stress intervals are selected.

The results of the second set of computations, in which 0.05 g load factor class intervals were used, are not nearly as accurate as those of the first set of computations. In Table VIII one observes that the calculated damage decreases significantly as one reduces the number of bits. This damage decrease is caused by the shifting of many cycles of ΔN_z to lower ΔN_z intervals because of the lack of alignment between digital and ΔN_z boundaries. This phenomena is caused by the basic nature of the digital recording technique, which is explained by the diagram in Figure 16 and the data in Table IX.

A digital recorder reads a continuous time history signal by sampling the signal at regular time intervals and then determining how many digital counts most closely represents the value of the signal. This is much the same procedure a person would use if he were measuring the distance between two points with a ruler graduated in 1/8-inch intervals, for example. Then the person would be instructed that he <u>may not interpolate</u>, and he must express the reading in terms of the <u>largest 1/8-inch interval that was exceeded</u>. Thus, when a digital recorder samples and digitizes a reading at time t, it indicates that the actual value of the data point is at least as large as the recorded digital level and that the data point value is less than the next higher digital level. In other words, a digital recorder categorizes the data into histograms having class interval boundaries defined by the digital count levels.

Referring to Figure 16, the point D, when digitized on the 11-bit scale, would be read as 25 counts; i.e., it is larger than 25 counts, yet less than 26 counts. Likewise on the 7-bit scale, point D would be read as 1 count.

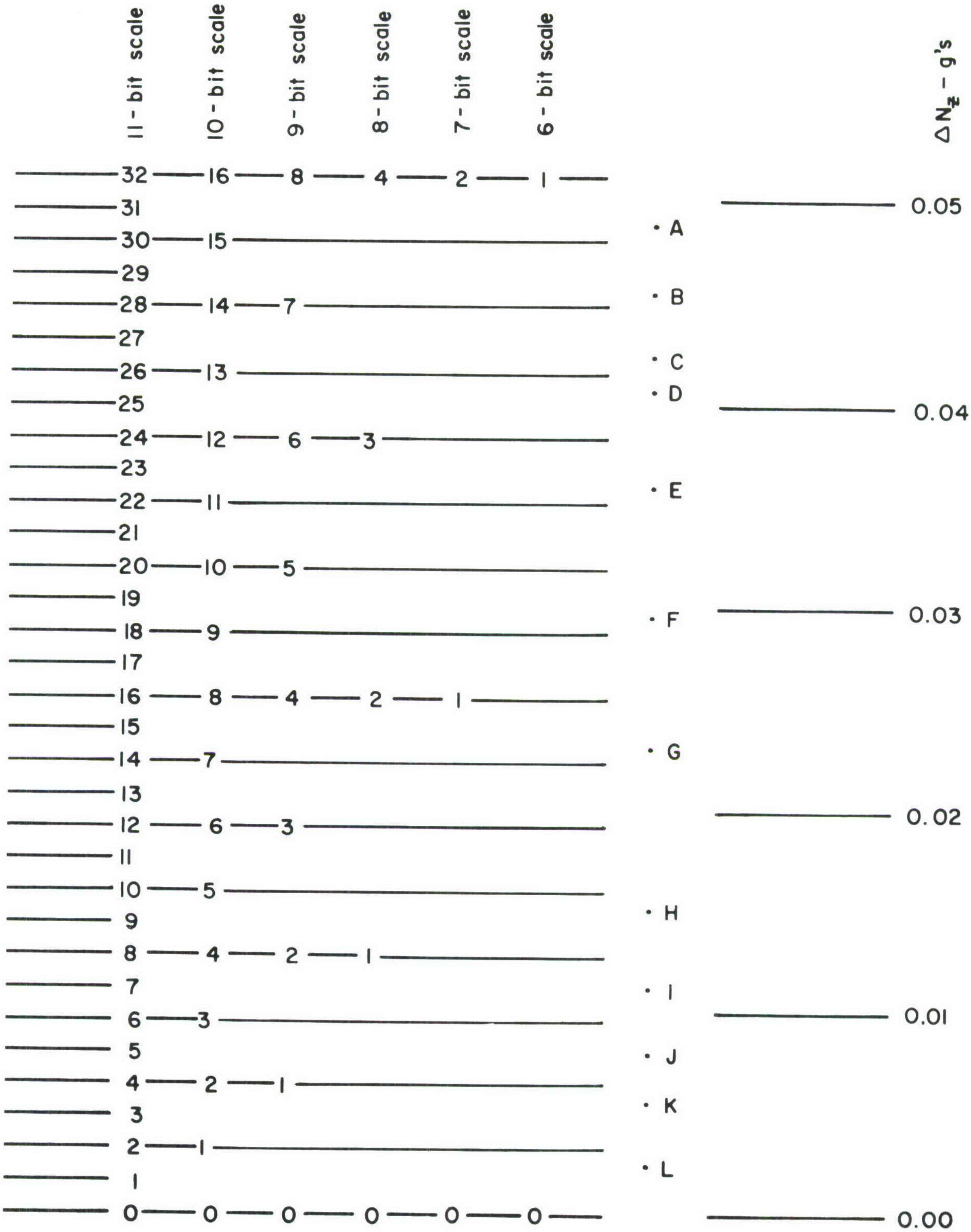

Figure 16. Relationship Between the True Magnitudes of Various Data Points, the Corresponding Digital Scales for Six Levels of Digital Resolution, and the Class Interval Boundaries of a ΔN_z Spectrum (Ref. Table IX)

TABLE IX

Digital Counts vs N_Z Class Intervals for Six Levels of Digital Resolution
(Ref. Figure 16)

Point	11-Bit	10-Bit	9-Bit	8-Bit	7-Bit	6-Bit
A-Counts	30	15	7	3	1	0
A-N_z	0.04	0.04	0.04	0.03	0.02	0
B-Counts	28	14	7	3	1	0
B-N_z	0.04	0.04	0.04	0.03	0.02	0
C-Counts	26	13	6	3	1	0
C-N_z	0.04	0.04	0.03	0.03	0.02	0
D-Counts	25	12	6	3	1	0
D-N_z	0.04	0.03	0.03	0.03	0.02	0
E-Counts	22	11	5	2	1	0
E-N_z	0.03	0.03	0.03	0.02	0.02	0
F-Counts	18	9	4	2	1	0
F-N_z	0.02	0.02	0.02	0.02	0.02	0
G-Counts	14	7	3	1	0	0
G-N_z	0.02	0.02	0.01	0.01	0	0
H-Counts	9	4	2	1	0	0
H-N_z	0.01	0.01	0.01	0.01	0	0
I-Counts	7	3	1	0	0	0
I-N_z	0.01	0	0	0	0	0
J-Counts	5	2	1	0	0	0
J-N_z	0	0	0	0	0	0
K-Counts	3	1	0	0	0	0
K-N_z	0	0	0	0	0	0
L-Counts	1	0	0	0	0	0
L-N_z	0	0	0	0	0	0

Using this technique, the twelve data points in Figure 16 were read according to each of the six digital scales and then the digital readings were converted to corresponding ΔN_z class interval values according to the ΔN_z scale at the right of Figure 16. The results of these readings and conversions are listed in Table IX. Thus, the cause for data points shifting to lower ΔN_z bands as the digital resolution is decreased, and the resultant damage decrease with decreased digital resolution (shown in Table VII) is an inherent phenomena in even an ideal digital system.

The foregoing example was a particularly severe one in that the N_z intervals were much smaller than those used in practice. Space prohibited the use of more realistic levels. The computations in Table VII used ΔN_z intervals of 0.05 g, whereas intervals of 0.01 were used in the example. Thus, as the ΔN_z intervals become more coarse, the effect of data points shifting with decreasing digital resolution is reduced.

SECTION IV

CONCLUSIONS AND RECOMMENDATIONS

A. Conclusions

The conclusions of this study are believed to be representative of the parameters studied during this program and should be sufficiently general for the intended purpose of the study. However, the shape of the S-N curve, the load factor spectrum, and the aircraft response are all capable of affecting the sensitivity of an aircraft response measurement to digital resolution, and hence for aircraft and environments that are significantly different from those used for these studies, different results may be obtained. The conclusions obtained from this study are as follows:

1. The effect of the alternating stress interval size on Miner's cumulative fatigue damage computation is much more pronounced than the mean stress interval size. For the range of stresses and materials analyzed on this program, the integration error in cumulative fatigue damage will be less than ±2% if the alternating and mean stress ranges are divided into at least 30 and 5 intervals, respectively.

2. The number of alternating stress intervals required to produce fatigue damage computations of a given accuracy decreases as the range from minimum to maximum mean stresses of an aircraft increases.

3. The inaccuracy of the damage computation increased as the notch sensitivity factor of 7075-T6 aluminum was increased from 4 to 6. This added error is due to the shifting of the damage density curve (Figure 5) to lower alternating stress levels, and hence larger errors were caused by the resulting integration over the more non-linear portion of the S-N curve.

4. The damage computations from a six-flight sample of B-58 data were relatively insensitive to digital resolution changes from 8 bits to 11 bits. Damage accuracy variations from one flight to another showed definite

degradation when digital resolution was decreased to 7 and 6 bits. This observation applies to the computations wherein the mean drift was ignored as well as to those for which corrections for mean drift were made.

5. Neglecting the correction for mean drift caused an average overestimation of fatigue damage by 16% for 11-bit data and 26% for 6-bit data. It is believed that these errors are representative of those that would be caused by instrumentation systems currently in use for flight loads programs on operational aircraft.

6. The decrease in digital resolution from 11 bits to 6 bits caused a significant increase in the number of low-magnitude load factor peaks in the ΔN_z spectrum. For some aircraft types this inaccuracy would not cause appreciable damage computation errors, but since one of the uses of the ASIP recorder will be to generate design criteria for future aircraft, reasonably accurate spectra should be generated. It is concluded that more consistently accurate ΔN_z data from one flight to another would be obtained if a digital resolution of at least 8 bits were used.

7. Definite benefits in data accuracy at relatively low-magnitude digital resolution levels can be obtained if the instrumentation system can be designed so that digital levels coincide with the class interval boundaries of a ΔN_z or stress spectrum. However, the trade-off in cost to develop such an ideal system probably will be prohibitive.

B. Recommendations

The following recommendations are made.

1. The ASIP recorder specifications should provide for a minimum resolution of 8 digital bits for all measurements.

2. The specification for the entire ASIP instrumentation system need not be overly concerned with system drift. Moderate care should be taken to control drift such that it is of the order of 2% of full scale, but since

drift correction methods are available, a cost penalty for less drift does not seem to be warranted.

3. In conducting cumulative fatigue damage computations wherein Miner's theory is used, it is recommended that the stress spectrum be divided into 30 alternating stress intervals and a minimum of 5 mean stress intervals if a computational accuracy of ±2% is desired.

REFERENCES

1. Anon, Air Force Aircraft Structural Integrity Program Requirements, ASD-TR-66-57, Aeronautical Systems Division, 7 April 1969.

2. Dominic, R. J., B-58 Lead-the-Force Flight Loads Program, Phase II, Interim Engineering Report UDRI TM 66-118, University of Dayton Research Institute, January 1967.

3. Kelly, L. G., Structural Flight Loads Data from B-52G Aircraft ASD-TR-62-634, Aeronautical Systems Division, December 1962.

4. Dominic, R. J., Evaluation of a Digital Data Compression Recorder, UDRI-TR-68-45, University of Dayton Research Institute, in publication.

5. Miner, M. A., "Cumulative Damage in Fatigue," J. Appl. Mech., Vol. 12, No. 1, September 1945.

6. Kaechele, L., Review and Analysis of Cumulative-Fatigue Damage Theories, RM-3650-PR, The Rand Corporation, August 1963.

7. Rice, S. O., "The Distribution of the Maxima of a Random Curve," American Journal of Mathematics, Vol. 61, 1939.

APPENDIX

S-N DATA

TABLE A-I

S-N Data for 7075-T6 Aluminum $K_T = 4$

SM	SA= 2500.	SA= 3000.	SA= 4000.	SA= 5000.	SA= 6000.	SA= 8000.	SA= 10000.	SA= 12000.	SA= 14000.	SA= 16000.
-10000.	1.000E 20	1.000E 20	1.000E 20	1.000E 20	1.000E 20	1.000E 20	1.000E 20	2.000E 06	6.530E 05	2.070E 05
-5000.	1.000E 20	1.000E 20	1.000E 20	1.000E 20	1.000E 20	10.000E 12	7.350E 05	3.750E 05	1.340E 05	5.530E 04
-2500.	1.000E 20	1.000E 20	1.000E 20	1.000E 20	1.000E 20	1.200E 07	7.050E 05	1.790E 05	6.900E 04	3.150E 04
0.	1.000E 20	1.000E 20	1.000E 20	1.000E 20	1.000E 20	2.750E 06	3.050E 05	9.300E 04	3.920E 04	1.960E 04
2500.	1.000E 20	1.000E 20	1.000E 20	1.000E 20	1.000E 20	8.600E 05	1.450E 05	5.350E 04	2.420E 04	1.280E 04
5000.	1.000E 20	1.000E 20	1.000E 20	1.000E 20	3.500E 07	3.350E 05	7.750E 04	3.290E 04	1.610E 04	9.000E 03
7500.	1.000E 20	1.000E 20	1.000E 20	1.000E 20	3.600E 06	1.410E 05	4.730E 04	2.200E 04	1.160E 04	6.780E 03
10000.	1.000E 20	1.000E 20	1.000E 20	1.150E 07	5.920E 05	7.250E 04	3.230E 04	1.580E 04	8.800E 03	5.270E 03
12500.	1.000E 20	1.000E 20	1.000E 20	1.300E 06	1.640E 05	4.700E 04	2.290E 04	1.180E 04	6.800E 03	4.250E 03
15000.	1.000E 20	1.000E 20	1.200E 07	2.460E 05	8.700E 04	3.420E 04	1.720E 04	9.250E 03	5.400E 03	3.520E 03
17500.	1.000E 20	1.000E 20	9.800E 05	1.260E 05	6.300E 04	2.600E 04	1.370E 04	7.580E 03	4.470E 03	3.020E 03
20000.	1.000E 20	1.000E 10	3.150E 05	8.570E 04	4.820E 04	2.130E 04	1.140E 04	6.400E 03	3.800E 03	2.660E 03
22500.	1.000E 20	6.100E 06	1.810E 05	6.750E 04	3.870E 04	1.820E 04	9.800E 03	5.570E 03	3.430E 03	2.400E 03
25000.	1.100E 08	1.690E 06	1.290E 05	5.600E 04	3.280E 04	1.600E 04	8.750E 03	5.080E 03	3.180E 03	2.210E 03
27500.	9.400E 06	7.900E 05	1.020E 05	4.900E 04	2.950E 04	1.450E 04	7.980E 03	4.700E 03	3.000E 03	2.070E 03
30000.	5.050E 06	5.120E 05	8.650E 04	4.500E 04	2.770E 04	1.330E 04	7.450E 03	4.430E 03	2.870E 03	1.950E 03
35000.	3.500E 06	4.000E 05	7.950E 04	4.180E 04	2.610E 04	1.220E 04	6.800E 03	4.000E 03	2.610E 03	1.780E 03
40000.	2.490E 06	3.330E 05	7.420E 04	3.900E 04	2.430E 04	1.110E 04	6.250E 03	3.700E 03	2.440E 03	1.660E 03
45000.	1.630E 06	2.600E 05	6.600E 04	3.570E 04	2.200E 04	1.010E 04	5.800E 03	3.470E 03	2.270E 03	1.530E 03
50000.	10.000E 05	1.940E 05	5.720E 04	3.180E 04	1.970E 04	9.200E 03	5.380E 03	3.270E 03	2.100E 03	1.400E 03

TABLE A-I, Continued

SM	SA= 18000.	SA= 20000.	SA= 24000.	SA= 28000.	SA= 32000.	SA= 36000.	SA= 40000.	SA= 50000.	SA= 60000.	SA= 70000.
-10000.	6.840E 04	2.920E 04	7.980E 03	2.200E 03	9.000E 02	4.250E 02	2.230E 02	5.950E 01	2.520E 01	1.310E 01
-5000.	2.430E 04	1.210E 04	3.720E 03	1.270E 03	5.450E 02	2.600E 02	1.420E 02	4.480E 01	2.110E 01	1.150E 01
-2500.	1.530E 04	8.400E 03	2.710E 03	10.000E 02	4.570E 02	2.320E 02	1.320E 02	4.120E 01	1.920E 01	1.070E 01
0.	1.020E 04	5.880E 03	2.090E 03	3.250E 02	4.100E 02	2.120E 02	1.230E 02	3.950E 01	1.850E 01	1.010E 01
2500.	7.100E 03	4.370E 03	1.680E 03	7.030E 02	3.700E 02	1.970E 02	1.160E 02	3.820E 01	1.790E 01	9.750E 00
5000.	5.270E 03	3.330E 03	1.400E 03	6.200E 02	3.400E 02	1.840E 02	1.100E 02	3.680E 01	1.740E 01	9.300E 00
7500.	4.110E 03	2.640E 03	1.180E 03	5.550E 02	3.170E 02	1.740E 02	1.050E 02	3.590E 01	1.690E 01	8.850E 00
10000.	3.320E 03	2.170E 03	1.030E 03	5.050E 02	2.960E 02	1.650E 02	1.000E 02	3.500E 01	1.650E 01	8.400E 00
12500.	2.720E 03	1.850E 03	8.950E 02	4.650E 02	2.790E 02	1.580E 02	9.600E 01	3.400E 01	1.610E 01	6.250E 00
15000.	2.290E 03	1.600E 03	8.050E 02	4.350E 02	2.640E 02	1.520E 02	9.250E 01	3.330E 01	1.580E 01	1.010E 00
17500.	1.990E 03	1.450E 03	7.400E 02	4.080E 02	2.520E 02	1.480E 02	8.930E 01	3.270E 01	1.560E 01	1.010E 00
20000.	1.770E 03	1.310E 03	6.900E 02	3.870E 02	2.400E 02	1.440E 02	8.700E 01	3.200E 01	1.540E 01	1.010E 00
22500.	1.620E 03	1.200E 03	6.550E 02	3.680E 02	2.320E 02	1.390E 02	8.450E 01	3.140E 01	1.000E 01	1.010E 00
25000.	1.510E 03	1.140E 03	6.300E 02	3.520E 02	2.230E 02	1.330E 02	8.250E 01	3.090E 01	1.010E 00	1.010E 00
27500.	1.430E 03	1.080E 03	6.030E 02	3.390E 02	2.140E 02	1.280E 02	8.000E 01	3.030E 01	1.010E 00	1.010E 00
30000.	1.380E 03	1.010E 03	5.360E 02	3.250E 02	2.050E 02	1.220E 02	7.730E 01	2.850E 01	1.010E 00	1.010E 00
35000.	1.250E 03	9.750E 02	5.000E 02	2.930E 02	1.850E 02	1.090E 02	7.080E 01	1.010E 00	1.010E 00	1.010E 00
40000.	1.130E 03	8.200E 02	4.370E 02	2.580E 02	1.590E 02	9.750E 01	5.950E 01	1.010E 00	1.010E 00	1.010E 00
45000.	1.010E 03	7.450E 02	3.780E 02	2.200E 02	1.330E 02	8.600E 00	1.010E 00	1.010E 00	1.010E 00	1.010E 00
50000.	8.800E 02	5.800E 02	2.800E 02	1.500E 02	7.000E 01	1.010E 00	1.010E 00	1.010E 00	1.010E 00	1.010E 00

TABLE A-II

S-N Data for 4130 Steel $K_T = 5$

SM	SA= 2000.	SA= 3000.	SA= 4000.	SA= 6000.	SA= 8000.	SA= 10000.	SA= 12000.	SA= 16000.	SA= 20000.	SA= 24000.
0.	1.100E 20	1.100E 20	1.100E 20	1.100E 20	3.000E 12	9.000E 10	10.000E 06	7.000E 05	2.500E 05	1.300E 05
4000.	1.100E 20	1.100E 20	1.100E 20	1.100E 20	2.000E 11	3.500E 09	4.500E 06	5.500E 05	2.000E 05	1.070E 05
8000.	1.100E 20	1.100E 20	1.100E 20	1.100E 20	1.000E 10	2.000E 08	2.350E 06	4.300E 05	1.600E 05	9.000E 04
12000.	1.100E 20	1.100E 20	1.100E 20	1.100E 20	5.000E 08	2.000E 07	1.350E 06	3.320E 05	1.300E 05	7.600E 04
16000.	1.100E 20	1.100E 20	1.100E 20	5.000E 12	4.200E 07	5.000E 06	8.620E 05	2.560E 05	1.100E 05	6.400E 04
20000.	1.100E 20	1.100E 20	1.100E 20	1.700E 10	8.400E 06	2.000E 06	6.000E 05	2.000E 05	9.200E 04	5.500E 04
24000.	1.100E 20	1.100E 20	1.100E 20	7.500E 07	3.000E 06	10.000E 05	4.350E 05	1.580E 05	7.750E 04	4.710E 04
28000.	1.100E 20	1.100E 20	5.500E 12	9.400E 06	1.420E 06	6.100E 05	3.250E 05	1.230E 05	6.600E 04	4.050E 04
32000.	1.100E 20	1.100E 20	1.500E 08	3.300E 06	8.600E 05	4.400E 05	2.500E 05	1.000E 05	5.750E 04	3.510E 04
36000.	1.100E 20	1.100E 20	1.130E 07	1.610E 06	5.800E 05	3.350E 05	1.980E 05	8.600E 04	5.000E 04	3.050E 04
40000.	1.100E 20	2.100E 07	4.000E 06	1.010E 06	4.600E 05	2.720E 05	1.600E 05	7.350E 04	4.300E 04	2.650E 04
44000.	2.500E 07	7.100E 06	2.200E 06	7.500E 05	3.730E 05	2.240E 05	1.340E 05	6.400E 04	3.700E 04	2.300E 04
48000.	10.000E 06	3.800E 06	1.450E 06	6.000E 05	3.150E 05	1.880E 05	1.140E 05	5.550E 04	3.250E 04	2.010E 04
52000.	6.000E 06	2.500E 06	1.130E 06	5.000E 05	2.680E 05	1.610E 05	9.950E 04	4.950E 04	2.850E 04	1.770E 04
56000.	4.450E 06	1.950E 06	9.600E 05	4.300E 05	2.300E 05	1.290E 05	8.900E 04	4.500E 04	2.500E 04	1.540E 04
60000.	3.600E 06	1.600E 06	8.200E 05	3.730E 05	2.020E 05	1.210E 05	7.800E 04	4.100E 04	2.200E 04	1.340E 04
64000.	3.000E 06	1.350E 06	7.300E 05	3.300E 05	1.800E 05	1.080E 05	7.000E 04	3.600E 04	1.950E 04	1.190E 04
68000.	2.550E 06	1.160E 06	6.600E 05	3.000E 05	1.600E 05	9.500E 04	6.400E 04	3.300E 04	1.700E 04	1.040E 04
72000.	2.200E 06	1.020E 06	6.000E 05	2.700E 05	1.460E 05	8.500E 04	5.750E 04	2.800E 04	1.500E 04	9.200E 03
80000.	1.700E 06	8.100E 05	5.100E 05	2.280E 05	1.190E 05	6.800E 04	4.700E 04	2.200E 04	1.200E 04	7.100E 03

TABLE A-II, Continued

SM	SA= 28000.	SA= 32000.	SA= 36000.	SA= 40000.	SA= 50000.	SA= 60000.	SA= 70000.	SA= 80000.	SA= 90000.	SA= 100000.
0.	7.600E 04	4.500E 04	3.000E 04	2.000E 04	7.600E 03	3.500E 03	1.700E 03	8.300E 02	4.300E 02	2.300E 02
4000.	6.300E 04	3.700E 04	2.530E 04	1.700E 04	6.600E 03	3.150E 03	1.500E 03	7.600E 02	3.800E 02	2.100E 02
8000.	5.300E 04	3.280E 04	2.180E 04	1.450E 04	5.850E 03	2.750E 03	1.330E 03	6.800E 02	3.450E 02	1.880E 02
12000.	4.500E 04	2.800E 04	1.860E 04	1.270E 04	5.180E 03	2.430E 03	1.180E 03	6.100E 02	3.100E 02	1.700E 02
16000.	3.850E 04	2.400E 04	1.600E 04	1.130E 04	4.550E 03	2.150E 03	1.060E 03	5.420E 02	2.810E 02	1.530E 02
20000.	3.300E 04	2.100E 04	1.400E 04	9.600E 03	4.000E 03	1.910E 03	9.400E 02	4.900E 02	2.580E 02	1.380E 02
24000.	2.840E 04	1.800E 04	1.200E 04	8.350E 03	3.550E 03	1.700E 03	8.400E 02	4.400E 02	2.340E 02	1.250E 02
28000.	2.460E 04	1.560E 04	1.060E 04	7.300E 03	3.150E 03	1.520E 03	7.600E 02	4.000E 02	2.130E 02	1.130E 02
32000.	2.140E 04	1.380E 04	9.230E 03	6.450E 03	2.790E 03	1.370E 03	6.900E 02	3.620E 02	1.950E 02	1.020E 02
36000.	1.860E 04	1.200E 04	8.150E 03	5.700E 03	2.500E 03	1.210E 03	6.200E 02	3.300E 02	1.780E 02	9.400E 01
40000.	1.620E 04	1.060E 04	7.200E 03	5.000E 03	2.200E 03	1.100E 03	5.600E 02	3.000E 02	1.610E 02	8.500E 01
44000.	1.420E 04	9.200E 03	6.400E 03	4.450E 03	2.000E 03	1.010E 03	5.200E 02	2.730E 02	1.500E 02	7.750E 01
48000.	1.240E 04	8.100E 03	5.600E 03	3.920E 03	1.800E 03	9.300E 02	4.750E 02	2.500E 02	1.370E 02	7.050E 01
52000.	1.100E 04	7.200E 03	4.950E 03	3.500E 03	1.630E 03	8.500E 02	4.350E 02	2.280E 02	1.250E 02	6.300E 01
56000.	9.700E 03	6.400E 03	4.400E 03	3.100E 03	1.460E 03	7.800E 02	4.000E 02	2.070E 02	1.120E 02	5.200E 01
60000.	8.500E 03	5.600E 03	3.900E 03	2.750E 03	1.300E 03	7.000E 02	3.600E 02	1.900E 02	9.800E 01	4.000E 01
64000.	7.500E 03	4.900E 03	3.460E 03	2.450E 03	1.170E 03	6.400E 02	3.230E 02	1.700E 02	8.100E 01	2.850E 01
68000.	6.600E 03	4.380E 03	3.080E 03	2.200E 03	1.030E 03	5.650E 02	2.900E 02	1.500E 02	6.450E 01	1.830E 01
72000.	5.850E 03	3.900E 03	2.750E 03	1.950E 03	9.100E 02	5.000E 02	2.550E 02	1.280E 02	4.930E 01	1.050E 01
80000.	4.600E 03	3.100E 03	2.200E 03	1.550E 03	7.100E 02	3.800E 02	1.900E 02	8.150E 01	1.700E 01	2.500E 00

TABLE A-III

S-N Data for 7075-T6 Aluminum $K_T = 6$

SM	SA= 2000.	SA= 2500.	SA= 3000.	SA= 4000.	SA= 5000.	SA= 6000.	SA= 8000.	SA= 10000.	SA= 12000.	SA= 14000.
-10000.	1.000E 20	1.000E 20	1.000E 20	1.000E 20	1.000E 20	1.000E 20	1.000E 20	1.000E 20	1.320E 06	3.630E 05
-5000.	1.000E 20	1.000E 20	1.000E 20	1.000E 20	1.000E 20	6.400E 07	3.100E 06	4.000E 05	1.020E 05	4.220E 04
-2500.	1.000E 20	1.000E 20	1.650E 11	4.000E 08	3.600E 07	7.550E 06	4.700E 05	1.030E 05	4.350E 04	2.160E 04
0.	1.200E 13	1.800E 10	1.370E 09	5.720E 07	6.550E 06	1.480E 06	1.570E 05	4.900E 04	2.510E 04	1.370E 04
2500.	4.100E 11	2.280E 09	1.860E 08	9.300E 06	1.140E 06	3.550E 05	7.950E 04	3.020E 04	1.640E 04	9.370E 03
5000.	1.400E 10	2.750E 08	3.150E 07	1.790E 06	3.500E 05	1.300E 05	4.650E 04	2.070E 04	1.170E 04	6.850E 03
7500.	8.450E 09	7.500E 07	6.650E 06	5.900E 05	1.700E 05	7.850E 04	3.230E 04	1.530E 04	8.580E 03	5.050E 03
10000.	2.720E 09	1.870E 07	1.660E 06	2.920E 05	1.020E 05	5.350E 04	2.300E 04	1.140E 04	6.550E 03	3.850E 03
12500.	9.450E 08	5.830E 06	1.010E 06	2.000E 05	7.600E 04	4.050E 04	1.730E 04	8.870E 03	5.030E 03	3.050E 03
15000.	3.440E 08	3.340E 06	7.350E 05	1.530E 05	6.300E 04	3.280E 04	1.380E 04	7.130E 03	3.950E 03	2.500E 03
17500.	1.320E 08	2.380E 06	5.740E 05	1.250E 05	5.250E 04	2.770E 04	1.150E 04	5.800E 03	3.550E 03	2.120E 03
20000.	7.000E 07	1.900E 06	4.700E 05	1.060E 05	4.650E 04	2.490E 04	1.000E 04	5.000E 03	2.900E 03	1.870E 03
22500.	3.700E 07	1.620E 06	4.090E 05	9.350E 04	4.300E 04	2.330E 04	9.300E 03	4.630E 03	2.720E 03	1.680E 03
25000.	2.150E 07	1.430E 07	3.740E 05	8.520E 04	4.030E 04	2.220E 04	8.950E 03	4.470E 03	2.610E 03	1.570E 03
27500.	1.520E 07	1.280E 06	3.570E 05	7.930E 04	3.830E 04	2.170E 04	8.800E 03	4.370E 03	2.530E 03	1.500E 03
30000.	1.220E 07	1.190E 06	3.370E 05	7.450E 04	3.680E 04	2.120E 04	8.800E 03	4.300E 03	2.370E 03	1.430E 03
35000.	9.230E 06	9.700E 05	2.850E 05	6.720E 04	3.400E 04	2.020E 04	8.530E 03	4.170E 03	2.320E 03	1.340E 03
40000.	7.450E 06	7.650E 05	2.360E 05	6.120E 04	3.190E 04	1.940E 04	8.310E 03	4.100E 03	2.230E 03	1.280E 03
45000.	5.400E 06	5.670E 05	1.910E 05	5.700E 04	3.070E 04	1.870E 04	8.200E 03	4.060E 03	2.170E 03	1.210E 03
50000.	3.220E 06	4.050E 05	1.520E 05	5.400E 04	3.010E 04	1.810E 04	8.100E 03	4.010E 03	2.100E 03	1.150E 03

TABLE A-III, Continued

SM	SA= 16000.	SA= 20000.	SA= 24000.	SA= 28000.	SA= 32000.	SA= 36000.	SA= 40000.	SA= 50000.	SA= 60000.	SA= 70000.
-10000.	1.230E 05	1.930E 04	4.830E 03	1.920E 03	9.000E 02	3.850E 02	2.000E 02	7.000E 01	2.590E 01	1.300E 01
-5000.	2.030E 04	6.380E 03	2.270E 03	1.110E 03	5.430E 02	2.600E 02	1.410E 02	4.550E 01	1.820E 01	8.500E 00
-2500.	1.220E 04	4.300E 03	1.630E 03	8.520E 02	4.230E 02	2.180E 02	1.230E 02	4.150E 01	1.590E 01	7.000E 00
0.	7.950E 03	3.080E 03	1.260E 03	6.600E 02	3.350E 02	1.800E 02	1.030E 02	3.420E 01	1.280E 01	5.460E 00
2500.	5.430E 03	2.330E 03	1.010E 03	5.250E 02	2.730E 02	1.510E 02	8.850E 01	2.870E 01	1.070E 01	4.230E 00
5000.	4.050E 03	1.800E 03	8.200E 02	4.280E 02	2.300E 02	1.280E 02	7.670E 01	2.430E 01	9.000E 00	3.130E 00
7500.	3.120E 03	1.410E 03	6.720E 02	3.470E 02	1.970E 02	1.120E 02	6.770E 01	2.080E 01	7.500E 00	2.310E 00
10000.	2.460E 03	1.130E 03	5.520E 02	2.920E 02	1.700E 02	9.850E 01	6.070E 01	1.830E 01	6.250E 00	1.630E 00
12500.	1.990E 03	9.300E 02	4.640E 02	2.530E 02	1.490E 02	8.790E 01	5.430E 01	1.580E 01	5.150E 00	1.090E 00
15000.	1.640E 03	7.650E 02	4.000E 02	2.210E 02	1.330E 02	7.920E 01	4.750E 01	1.350E 01	4.130E 00	1.010E 00
17500.	1.380E 03	6.500E 02	3.480E 02	1.930E 02	1.160E 02	7.080E 01	4.300E 01	1.130E 01	2.900E 00	1.010E 00
20000.	1.180E 03	5.580E 02	3.030E 02	1.720E 02	1.030E 02	6.370E 01	3.800E 01	9.500E 00	1.900E 00	1.010E 00
22500.	1.060E 03	4.950E 02	2.740E 02	1.540E 02	9.150E 01	5.640E 01	3.300E 01	7.500E 00	1.150E 00	1.010E 00
25000.	9.870E 02	4.530E 02	2.490E 02	1.390E 02	8.290E 01	5.020E 01	2.830E 01	5.500E 00	1.010E 00	1.010E 00
27500.	9.350E 02	4.250E 02	2.280E 02	1.270E 02	7.450E 01	4.360E 01	2.360E 01	3.700E 00	1.010E 00	1.010E 00
30000.	8.950E 02	4.050E 02	2.090E 02	1.190E 02	6.720E 01	3.680E 01	1.880E 01	2.350E 00	1.010E 00	1.010E 00
35000.	8.520E 02	3.650E 02	1.760E 02	9.580E 01	5.200E 01	2.420E 01	1.030E 01	1.010E 00	1.010E 00	1.010E 00
40000.	8.000E 02	3.300E 02	1.450E 02	6.850E 01	3.200E 01	1.300E 01	3.850E 00	1.010E 00	1.010E 00	1.010E 00
45000.	7.400E 02	2.740E 02	1.050E 02	3.950E 01	1.370E 01	3.610E 00	1.010E 00	1.010E 00	1.010E 00	1.010E 00
50000.	6.800E 02	2.100E 02	5.900E 01	1.350E 01	2.000E 00	1.010E 00	1.010E 00	1.010E 00	1.010E 00	1.010E 00

Unclassified
Security Classification

DOCUMENT CONTROL DATA - R&D

(Security classification of title, body of abstract and indexing annotation must be entered when the overall report is classified)

1. ORIGINATING ACTIVITY (Corporate author) University of Dayton Research Institute 300 College Park Dayton, Ohio 45409	2a. REPORT SECURITY CLASSIFICATION Unclassified 2b. GROUP

3. REPORT TITLE

Sensitivity of Fatigue Damage Calculations to the Stress Increment Size and Digital Resolution of Load Factor Data

4. DESCRIPTIVE NOTES (Type of report and inclusive dates)

Final Technical Report, 1 February 1969 through 1 April 1969

5. AUTHOR(S) (Last name, first name, initial)

Roth, George J.

6. REPORT DATE	7a. TOTAL NO. OF PAGES	7b. NO. OF REFS
September 1969	59	7

8a. CONTRACT OR GRANT NO. F33657-67-C-0140	9a. ORIGINATOR'S REPORT NUMBER(S)
b. PROJECT NO. Amendment No. P003	
c.	9b. OTHER REPORT NO(S) (Any other numbers that may be assigned this report) ASD-TR-69-105
d.	

10. AVAILABILITY/LIMITATION NOTICES

This document is subject to special export controls and each transmittal to foreign governments or foreign nationals may be made only with prior approval of the Deputy for Engineering, Aeronautical Systems Division, Wright-Patterson AFB, Ohio

11. SUPPLEMENTARY NOTES	12. SPONSORING MILITARY ACTIVITY
	Deputy for Engineering Aeronautical Systems Division Wright-Patterson AFB, Ohio 45433

13. ABSTRACT

Fatigue damage calculations using Miner's cumulative damage rule were performed to determine the trade-off relationship between the number of mean and alternating stress intervals used to represent a load spectrum. Results indicate that if more than 5 mean stress intervals and more than 30 alternating stress intervals are used, the error in the calculations will be less than 2%.

Also presented are results showing the effect that the number of digital binary bits used to represent loads data has on the calculated fatigue damage. These results indicate that the minimum resolution for the ASIP recorder should be 8 digital bits.

(This abstract is subject to special export controls and each transmittal to foreign governments or foreign nationals may be made only with prior approval of the Deputy for Engineering, Aeronautical Systems Division, Wright-Patterson Air Force Base, Ohio 45433.)

DD FORM 1 JAN 64 1473

Unclassified
Security Classification

14. KEY WORDS	LINK A		LINK B		LINK C	
	ROLE	WT	ROLE	WT	ROLE	WT
ASIP Recorder Specifications						
Digital Resolution						
Flight Loads						
Cumulative Fatigue Damage						
Miner's Theory						

INSTRUCTIONS

1. ORIGINATING ACTIVITY: Enter the name and address of the contractor, subcontractor, grantee, Department of Defense activity or other organization *(corporate author)* issuing the report.

2*a*. REPORT SECURITY CLASSIFICATION: Enter the overall security classification of the report. Indicate whether "Restricted Data" is included. Marking is to be in accordance with appropriate security regulations.

2*b*. GROUP: Automatic downgrading is specified in DoD Directive 5200.10 and Armed Forces Industrial Manual. Enter the group number. Also, when applicable, show that optional markings have been used for Group 3 and Group 4 as authorized.

3. REPORT TITLE: Enter the complete report title in all capital letters. Titles in all cases should be unclassified. If a meaningful title cannot be selected without classification, show title classification in all capitals in parenthesis immediately following the title.

4. DESCRIPTIVE NOTES: If appropriate, enter the type of report, e.g., interim, progress, summary, annual, or final. Give the inclusive dates when a specific reporting period is covered.

5. AUTHOR(S): Enter the name(s) of author(s) as shown on or in the report. Enter last name, first name, middle initial. If military, show rank and branch of service. The name of the principal author is an absolute minimum requirement.

6. REPORT DATE: Enter the date of the report as day, month, year; or month, year. If more than one date appears on the report, use date of publication.

7*a*. TOTAL NUMBER OF PAGES: The total page count should follow normal pagination procedures, i.e., enter the number of pages containing information.

7*b*. NUMBER OF REFERENCES: Enter the total number of references cited in the report.

8*a*. CONTRACT OR GRANT NUMBER: If appropriate, enter the applicable number of the contract or grant under which the report was written.

8*b*, 8*c*, & 8*d*. PROJECT NUMBER: Enter the appropriate military department identification, such as project number, subproject number, system numbers, task number, etc.

9*a*. ORIGINATOR'S REPORT NUMBER(S): Enter the official report number by which the document will be identified and controlled by the originating activity. This number must be unique to this report.

9*b*. OTHER REPORT NUMBER(S): If the report has been assigned any other report numbers *(either by the originator or by the sponsor)*, also enter this number(s).

10. AVAILABILITY/LIMITATION NOTICES: Enter any limitations on further dissemination of the report, other than those imposed by security classification, using standard statements such as:

(1) "Qualified requesters may obtain copies of this report from DDC."

(2) "Foreign announcement and dissemination of this report by DDC is not authorized."

(3) "U. S. Government agencies may obtain copies of this report directly from DDC. Other qualified DDC users shall request through

____ ."

(4) "U. S. military agencies may obtain copies of this report directly from DDC. Other qualified users shall request through

____ ."

(5) "All distribution of this report is controlled. Qualified DDC users shall request through

____ ."

If the report has been furnished to the Office of Technical Services, Department of Commerce, for sale to the public, indicate this fact and enter the price, if known.

11. SUPPLEMENTARY NOTES: Use for additional explanatory notes.

12. SPONSORING MILITARY ACTIVITY: Enter the name of the departmental project office or laboratory sponsoring *(paying for)* the research and development. Include address.

13. ABSTRACT: Enter an abstract giving a brief and factual summary of the document indicative of the report, even though it may also appear elsewhere in the body of the technical report. If additional space is required, a continuation sheet shall be attached.

It is highly desirable that the abstract of classified reports be unclassified. Each paragraph of the abstract shall end with an indication of the military security classification of the information in the paragraph, represented as *(TS)*, *(S)*, *(C)*, or *(U)*.

There is no limitation on the length of the abstract. However, the suggested length is from 150 to 225 words.

14. KEY WORDS: Key words are technically meaningful terms or short phrases that characterize a report and may be used as index entries for cataloging the report. Key words must be selected so that no security classification is required. Identifiers, such as equipment model designation, trade name, military project code name, geographic location, may be used as key words but will be followed by an indication of technical context. The assignment of links, rules, and weights is optional.